Pergamon

Geochimica et Cosmochimica Acta, Vol. 68, No. 22, pp. 4687-4703, 2004

0016-7037/04 $30.00 + .00

doi:10.1016/j.gca.2004.04.019

CO_2 solubility in dacitic melts equilibrated with H_2O-CO_2 fluids: Implications for modeling the solubility of CO_2 in silicic melts

HARALD BEHRENS,[1,*] SUSANNE OHLHORST,[1] FRANCOIS HOLTZ,[1] and MICHEL CHAMPENOIS[2]

[1]Institut für Mineralogie, Uni Hannover, Welfengarten 1, D-30167 Hannover, Germany
[2]CNRS-CRPG, B.P. 20, F-54501 Vandoeuvre les Nancy, France

(*Received April* 28, 2003; *accepted in revised form April* 28, 2004)

Abstract—The solubility of CO_2 in dacitic melts equilibrated with H_2O-CO_2 fluids was experimentally investigated at 1250°C and 100 to 500 MPa. CO_2 is dissolved in dacitic glasses as molecular CO_2 and carbonate. The quantification of total CO_2 in the glasses by mid-infrared (MIR) spectroscopy is difficult because the weak carbonate bands at 1430 and 1530 cm^{-1} can not be reliably separated from background features in the spectra. Furthermore, the ratio of $CO_{2,mol}$/carbonate in the quenched glasses strongly decreases with increasing water content. Due to the difficulties in quantifying CO_2 species concentrations from the MIR spectra we have measured total CO_2 contents of dacitic glasses by secondary ion mass spectrometry (SIMS).

At all pressures, the dependence of CO_2 solubility in dacitic melts on $x^{fluid}_{CO_{2,total}}$ shows a strong positive deviation from linearity with almost constant CO_2 solubility at $x^{fluid}_{CO_2} > 0.8$ (maximum CO_2 solubility of 795 ± 41, 1376 ± 73 and 2949 ± 166 ppm at 100, 200 and 500 MPa, respectively), indicating that dissolved water strongly enhances the solubility of CO_2. A similar nonlinear variation of CO_2 solubility with $x^{fluid}_{CO_2}$ has been observed for rhyolitic melts in which carbon dioxide is incorporated exclusively as molecular CO_2 (Tamic et al., 2001). We infer that water species in the melt do not only stabilize carbonate groups as has been suggested earlier but also CO_2 molecules.

A thermodynamic model describing the dependence of the CO_2 solubility in hydrous rhyolitic and dacitic melts on T, P, f_{CO_2} and the mol fraction of water in the melt (x_{water}) has been developed. An exponential variation of the equilibrium constant K_1 with x_{water} is proposed to account for the nonlinear dependence of $x^{melt}_{CO_{2,total}}$ on $x^{fluid}_{CO_2}$. The model reproduces the CO_2 solubility data for dacitic melts within ±14% relative and the data for rhyolitic melts within 10% relative in the pressure range 100–500 MPa (except for six outliers at low $x^{fluid}_{CO_2}$). Data obtained for rhyolitic melts at 75 MPa and 850°C show a stronger deviation from the model, suggesting a change in the solubility behavior of CO_2 at low pressures (a Henrian behavior of the CO_2 solubility is observed at low pressure and low H_2O concentrations in the melt). We recommend to use our model only in the pressure range 100–500 MPa and in the $x^{fluid}_{CO_2}$ range 0.1–0.95. The thermodynamic modeling indicates that the partial molar volume of total CO_2 is much lower in rhyolitic melts (31.7 cm^3/mol) than in dacitic melts (46.6 cm^3/mol). The dissolution enthalpy for CO_2 in hydrous rhyolitic melts was found to be negligible. This result suggests that temperature is of minor importance for CO_2 solubility in silicic melts.

1. INTRODUCTION

Volatiles dissolved in silicate melts influence dramatically the chemical and physical properties of magmas. Because of its high solubility in silicate melts, water is of particular interest for understanding properties of magmas. CO_2 is the second most abundant volatile in natural magmas. Although CO_2 is usually subordinate in concentration in silicic magmas, it is often the first component to reach saturation due to its low solubility in the melt. Even small amounts of dissolved CO_2 in water bearing melts shift the fluid saturation limit to higher pressures and thus greater depth (Holloway, 1976). Because vesiculation, initiated by exsolution of CO_2-H_2O-bearing fluids from the melt, is the driving force in many eruptive situations, it is important to investigate the saturation limit of fluids in the system C-H-O.

Similar to H_2O, CO_2 dissolves in silicate glasses and melts in form of at least two different species, as an unreacted molecular species (CO_2 molecules, hereafter referred to as $CO_{2,mol}$) and as species formed by reaction between molecular species and the silicate framework (carbonate groups). Whereas water speciation in glasses depends mainly on the total water content but only weakly on anhydrous composition (e.g., Silver et al., 1990; Behrens et al., 1996), the speciation of CO_2 is found to be independent on total CO_2 concentration but varies strongly with anhydrous composition of the glass (Fine and Stolper, 1985; Blank and Brooker, 1994; Brooker et al., 2001). In highly polymerized rhyolitic glasses CO_2 is incorporated exclusively as molecular CO_2 (e.g., Blank et al., 1993; Tamic et al., 2001), whereas only carbonate is present in more depolymerized glasses (Blank and Brooker, 1994). Glasses of intermediate compositions such as dacite, andesite and phonolite contain both types of species (Blank and Brooker, 1994; King and Holloway, 2002; Morizet et al., 2002).

Although CO_2 solubility data (if not specified otherwise, the term CO_2 refers to the total carbon dioxide) are available for a variety of natural and synthetic melt compositions (Mysen et al., 1975, 1976; Blank and Brooker, 1994; Dixon et al., 1995; Jakobsson, 1997; Brooker et al., 1999; Tamic et al., 2001; King and Holloway, 2002; King et al., 2002; Morizet et al., 2002), general models to predict the solubility of CO_2 in silicate melts

* Author to whom correspondence should be addressed (h.behrens@mineralogie.uni-hannover.de).

of mafic to silicic compositions (Spera and Bergman, 1980; Papale, 1999; Brooker et al., 2001) have large errors. This is due mainly to the uncertainty of the input data for the thermodynamic models. Especially, the early studies on CO_2 solubility in silicate melts suffer from imprecise analytical techniques.

CO_2 solubility in melts equilibrated with mixed H_2O-CO_2 fluids was investigated only in a few studies. In the pioneering works of Mysen et al. (1975, 1976), the highest CO_2 solubilities in andesitic, basaltic and albitic compositions were not found in melts in equilibrium with pure CO_2 fluids but for fluids with mole fractions of CO_2 ($x_{CO_2}^{fluid}$) of 0.6–0.7. Mysen et al. (1975, 1976) suggested that the formation of OH groups depolymerizes the melt structure, resulting in an increase of carbonate groups in the melt. However, as discussed by Tingle (1987), there may be substantial errors with the ^{14}C β-track autoradiography which was used by Mysen et al. (1975, 1976) to determine carbon quantitatively. In more recent studies, IR and NMR spectroscopy was used to measure CO_2 speciation and concentration in glasses. Rhyolitic compositions (containing only molecular CO_2) were examined by Blank et al. (1993) at 75 MPa and 850°C, and by Tamic et al. (2001) at 200 and 500 MPa and 800 and 1100°C. Basaltic compositions (containing only carbonate) were studied by Dixon et al. (1995) at 1200°C and pressures up to 98 MPa. To our knowledge, the effect of water on CO_2 speciation in glasses containing both $CO_{2,mol}$ and carbonate groups has been systematically investigated only in the studies of Kohn and Brooker (1994) and King and Holloway (2002) using samples synthesized at higher pressures in piston cylinder apparatus. Using ^{13}C MAS NMR spectroscopy, Kohn and Brooker (1994) found a maximum in the ratio of $CO_{2,mol}$/carbonate at a water content of 1–2 wt% in albitic and jadeitic glasses. On the other hand, IR spectroscopy on andesitic glasses showed a continuous decrease of $CO_{2,mol}$/carbonate with increasing water content of the melt from 0 to 3.4 wt% (King and Holloway, 2002).

In this paper, we report new experimental results on the solubility of CO_2 in dacitic melts in equilibrium with mixed H_2O-CO_2 fluids at 100, 200 and 500 MPa and 1250°C. To understand the solubility behavior of CO_2 in the melts, we have also examined the effect of water on the speciation of CO_2 in the quenched dacitic glasses using IR micro-spectroscopy. However, because the quantification of carbonate concentration in the glass by IR spectroscopy was found to be too imprecise, we applied secondary ion mass spectrometry (SIMS) to measure quantitatively the total CO_2 concentration in the samples. On the basis of the new solubility and speciation data for dacitic composition and data for rhyolitic composition from previous studies, a thermodynamic model is proposed to describe the dependence of the CO_2 solubility in silicic melts (rhyolite to dacite) on temperature, pressure, fugacity of CO_2 (f_{CO_2}) and the water content in the melt.

2. EXPERIMENTAL

2.1. Starting Material

The starting composition was a synthetic dry glass with a composition close to the bulk composition of the dacite of the Unzen Volcano, Japan (Chen et al., 1993). The homogenous dry glass was synthesized by melting oxides and carbonates at 1600°C for more than 4 h, grinding and remelting for additional 4 h at the same temperature. The composition of the glass, determined by electron microprobe, is given in Table 1 (average analysis using a Cameca microprobe, with 15 kV accelerating voltage, 5 nA beam current and a defocused beam with 10–30 μm in diameter). On an iron-free basis the dacite has a ratio of nonbridging oxygen to tetrahedrally coordinated cations (NBO/T) of 0.108.

Table 1. Composition of the starting glass (in wt%).

Element	DC dacite
SiO_2	65.84
TiO_2	0.66
Al_2O_3	15.44
FeO	4.73
MnO	0.07
MgO	2.14
CaO	4.89
Na_2O	3.68
K_2O	2.55
H_2O[a]	0.020

[a] The water content was derived from the peak height of the IR absorption band at 3550 cm^{-1} using a molar absorption coefficient of 62 $L \cdot mol^{-1} \cdot cm^{-1}$ from Stolper (1982) for silicate glasses.

2.2. Solubility Experiments and Synthesis of Standards for SIMS

In the solubility experiments single glass pieces of 18 to 75 mg were loaded together with distilled H_2O and a CO_2 source (oxalic acid dihydrate or anhydrous oxalic acide) in $Au_{80}Pd_{20}$ capsules. Then the capsules were welded shut while cooling the capsules with a water-soaked and frozen tissue to avoid water or CO_2 loss. The total amount of fluid always was higher than the expected volatile solubility. Single glass pieces were used to avoid bubbles within the melt which may not escape during experiment due to high melt viscosity. Such bubbles containing fluids may be formed when using glass powder. Several capsules were processed simultaneously in a vertically oriented internally heated pressure vessel (IHPV) at 1250°C (temperature far above the liquidus) and pressures of 100, 200 or 500 MPa. Run duration was 68 to 137 h, which is long enough for the small samples (typically $1 \times 3 \times 4$ mm) to allow equilibrium distribution of H_2O and a CO_2 in the melt, considering the diffusivity of these volatiles at 1250°C (Watson, 1994; Zhang and Behrens, 2000). At the end of the run the melts were rapidly quenched to glass by dropping off the capsule assemblage into the cold part of the furnace (cooling rate of −150°C/s). The detailed description of the IHPV and of the rapid quench system used for the experiments is given by Berndt et al. (2002). After the run the fluid composition in each capsule was determined by gravimetry (see Tamic et al. 2001).

The standards for the ion microprobe were synthesized at 1250°C and 500 MPa in the IHPV using dacitic glass powder (400–500 mg), water and silver oxalate as a CO_2 source (Table 2). The silver oxalate was isolated from the external capsule wall by wrapping it into an additional $Au_{80}Pd_{20}$ foil to avoid alloying of silver with the $Au_{80}Pd_{20}$ capsule, which can lead to a leakage. The amount of added H_2O and a CO_2 (Table 2) was below the solubility of these volatiles for these conditions. Thus, the formation of bubbles in the run products was avoided, even if glass powder was used as starting material. Water and glass powder were filled in two portions into the $Au_{80}Pd_{20}$ capsules, which subsequently were welded shut while cooling the capsules. To decompose the silver oxalate and to ensure a homogeneous CO_2 and water distribution, the capsules were stored horizontally for more than 8 h at 200°C in an oven.

Both the solubility experiments and the synthesis of glass standards were performed at intrinsic oxygen fugacities (buffered by the IHPV). At 1250°C, the oxygen fugacity corresponds to that buffered by the QFM assemblage (quartz-fayalite-magnetite) + 4.7 log units if capsules are water-saturated (pure H_2O-fluid). No iron loss by diffusion into the $Au_{80}Pd_{20}$ capsule is observed at this oxidizing oxygen fugacity (Berndt et al., 2002).

Table 2. Synthesis conditions and analytical results for the SIMS standards.[a]

	DC186	DC182	DC184
mg glass loaded	400.11	498.00	469.59
mg H_2O loaded	0.00	10.24	27.30
mg $Ag_2C_2O_4$ loaded	2.33	1.75	1.33
wt% H_2O in glass by mass balance	0.00	2.02	5.49
ppm CO_2 in glass by mass balance	1633	966	750
Run conditions		T = 1250°C, P = 500 MPa	
Run duration	68.2 h	17.7 h	65.4 h
mg glass used for CO_2 titration	258.68	307.60	362.10
ppm CO_2 by CO_2 titration	2544 ± 103	1364 ± 55	1316 ± 53
wt% water by	(t) 0.51 ± 0.06	(t) 2.21 ± 0.06	(c) 5.25 ± 0.09
NIR spectroscopy	(b) 0.53 ± 0.06	(b) 2.18 ± 0.06	(b) 6.49 ± 0.10

[a] Two sections for IR spectroscopy and SIMS were taken from the top (t), the center (c) or the bottom (b) of the glass pieces (top and bottom correspond to positions of the hanging capsule during synthesis). Total water content was calculated from peak heights of the NIR combination bands using the calibration of Ohlhorst et al. (2001).

3. ANALYTICAL

3.1. Karl-Fischer Titration (KFT)

The water content of glasses (C_{water}) from the solubility experiments were measured after thermal extraction using Karl-Fischer titration (Behrens, 1995). Single wafers of 10–20 mg were wrapped tightly in a Pt foil to avoid explosion during heating. To account for unextracted water in the samples after analysis, 0.13 ± 0.07 wt% H_2O were added to the quantity measured by KFT. This value was found to be typical for polymerized rhyolitic glasses (Leschik et al., 2004) as well as for depolymerized soda-lime silicate glasses (Behrens and Stuke, 2003).

3.2. CO_2 Titration

The concentration of CO_2 in glasses used as SIMS standards was determined by pyrolysis and subsequent coulometric titration (Deltromat 500, Deltronic). The method is based on the quantitative reaction of CO_2 with an alkaline (pH ~10) barium perchlorate solution: $Ba^{2+} + CO_2 + 2\ OH^- = BaCO_3 + H_2O$, resulting in a decrease of the pH value of the solution. To compensate the change of the pH value, OH^- is generated by electrolysis (coulometric titration): $2H_2O + 2\ e^- = 2OH^- + H_2$. The amount of CO_2 which reacted with the $Ba(ClO_4)_2$ solution can be directly calculated from the charge needed to generate hydroxyl ions (1 coulomb corresponds to 0.228 mg CO_2). A detailed description of the method is given in Behrens et al. (2004).

The sample is heated in a combustion tube to 1200°C to extract CO_2. This CO_2 is transported by an air stream to the titration cell connected with the coulometer electronics. The air stream was previously purified by oxidizing hydrocarbons in an oven at 800°C and adsorbing all CO_2 in a trap with soda lime pellets.

For a typical measurement duration of 90–120 s the background CO_2 value is 5.5 ± 2.2 μg. Based on 30 repeated measurements of rock powders with known carbon contents, the maximum uncertainty is estimated to be ±12.8 μg CO_2 (180–540 μg CO_2 were released from the samples, see Table 2). To obtain measurements with a precision better than 5% relative, sample weights of more than 100 mg at 2500 ppm CO_2 or 250 mg at 1000 ppm CO_2 are needed.

CO_2 bulk analysis may suffer from at least three sources of error: (i) CO_2 trapped in bubbles, (ii) carbon species adsorbed on the glass surface, and (iii) unextracted CO_2 in the glasses after analysis due to a too low temperature of combustion (Blank, 1993; King et al., 2002; Behrens et al., 2004).

To (i): Bubbles were not found in the experimental products because the charges were undersaturated with respect to both the H_2O and CO_2.

To (ii): Our analytical procedure involves a single heating step and, therefore, we can not distinguish carbon species adsorbed on the glass surface from those dissolved in the glass. No CO_2 was detected by IR spectroscopy on polished fragments of the starting glass. On the other hand, CO_2 titration of the powdered starting glass yields a CO_2 content of 81–143 ppm. We attribute this concentration of CO_2 as a carbon contamination adsorbed on the surface of the glass powder. The quantity of adsorbed CO_2 is similar to that found by Blank (1993) for rhyolitic glasses (34–165 ppm) using incremental heating to 600°C and subsequent CO_2 manometry.

To (iii): After CO_2 titration a foamy glass is obtained in which bubble-free volumes are too small to be analyzed by micro-beam techniques. Hence, no direct information is available about unextracted CO_2 after titration for dacitic glasses. We assume that the quantity of unextracted CO_2 is similar to that in rhyolitic glasses. Using IR microspectroscopy, 230 ± 28 ppm of unextracted CO_2 were found in decarbonated rhyolitic glasses after remelting at 1200°C and 500 MPa (Behrens et al., 2004).

We conclude that the adsorbed CO_2 on the surface is approximately compensating the unextracted CO_2 after analysis and did not correct the measured CO_2 concentrations in the standards. The error of this approach is roughly ± 200 ppm.

3.3. IR-Spectroscopy

Doubly polished glass plates of 130–230 μm thickness were prepared from solubility samples for MIR spectroscopy to investigate CO_2 speciation. Two fragments were collected from each SIMS standard in a distance of 10 mm or more to check the homogeneity and the composition of the glass batches. Total water content was measured on thick sections (ca. 0.5 mm) by NIR spectroscopy using the absorption coefficients determined by Ohlhorst et al. (2001) for the composition used in this study. The thickness of each glass plate was measured with a digital micrometer (Mitutoyo; precision ±2μm).

IR spectra were recorded with a Bruker IFS 88 FTIR spectrometer coupled with a microscope IR-Scope II (Operation conditions: MCT narrow range detector for both MIR and NIR; globar light source and KBr beamsplitter for MIR; tungsten lamp and CaF_2 beamsplitter for NIR). Spectral resolution was 1 cm^{-1} in MIR and 4 cm^{-1} in NIR. To minimize effects of varying CO_2 contents in the atmosphere, the sample stage of the IR microscope was shielded and purged with dry air (Tamic et al., 2001). Typically 20 scans were sufficient to obtain MIR spectra with a good signal/noise ratio. Short times between measurement of background spectra and sample spectra lower the error due to changes of CO_2 concentrations in the air stream. Longer measurements with up to 500 scans do not enhance significantly the precision of the spectra. Only one or two sample spectra were recorded after background measurement.

To quantify the variation of CO_2 in the beam path, we have compared in total 200 spectra collected without sample. These spectra were recorded in two ways over a period of several days: (1) series of 10 to 110 spectra were successively measured without opening the sample chamber of the IR microscope; (2) one or several blanc spectra were collected directly after a sample spectrum. At our measurement conditions, the intensity of the atmospheric CO_2 doublet at ~2350 cm^{-1} varied randomly with time by ±0.008 absorbance units and ±0.40 integral absorbance units (1 σ values). The corresponding variation of CO_2 content, e.g., ±8 ppm (peak height) or ±27 ppm (peak area) for

a 100 μm thick sample, is considered to be the precision of CO_2 absorbance measurement.

3.4. Secondary Ion Mass Spectrometry (SIMS)

In SIMS, a beam of ions is accelerated and focused onto the surface of a sample. The incoming ions sputter atoms from the surface of the sample. Some of these atoms are ionized (secondary ions) in the process and are analyzed by mass spectrometry. Historically, the ion probe measurements of volatiles have suffered from high backgrounds and poor detection limits, particularly for hydrogen and carbon (Ihinger et al., 1994). However, due to technical improvements in the last years, SIMS has become a powerful micro-analytical tool for precise measurements of the abundance and isotopic compositions of volatiles in silicate minerals and glasses (Deloule et al., 1995; Hanon et al., 1998; Hauri et al., 2002).

The reproducibility of the absolute intensities of secondary ions detected by SIMS in general is low. Hence, it is convenient to measure the ratio of the peak intensity of the isotope of interest to that of another isotope with well known concentration (e.g., ^{28}Si in silicates, e.g., Reed, 1989). The so-defined ion yield for each isotope depends not only upon the properties of the isotope itself (mainly the ionization potential) but also on the matrix. Matrix effects are especially large for hydrogen incorporated in silicate glasses but noticeable variations of the ion yield with composition are observed also for carbon (Hauri et al., 2002). Hauri et al. suggested that in their SIMS measurements the matrix effects for carbon is correlated with the ratio of $Na_2O/(Na_2O + CaO)$. To avoid matrix effects we have used standards of same bulk composition as used in the solubility experiments. Because dissolved water may also have a large effect on the ion yield in SIMS (Brenan et al., 1995; Wiedenbeck et al., 2001) we have synthesized standards with various water contents.

3.5. Sample Preparation for SIMS

Glass fragments used for SIMS were always taken directly adjacent to samples used for IR spectroscopy. Samples for SIMS were mounted with a resin in small holes drilled into a glass slide. Polishing the slices with diamond paste can lead to a carbon contamination on the surface. To avoid this contamination the slices were cleaned with distilled water in an ultrasonic bath and repolished with an alumina paste (a layer of $\sim$2 μm thickness was removed). After the first measurements we repolished the sample with a cerium oxide paste to ensure that there was no contamination from carbon. After polishing the samples were coated with gold.

3.6. Measurement Conditions

The total ^{12}C concentration in the glasses was measured with the ims 1270 ion microprobe at the CRPG in Nancy (France). Carbon forms negative ions readily and SIMS is an effective method for ^{12}C isotope measurement (e.g., McKeegan et al., 1985; Zinner et al., 1989). A primary beam of $^{133}Cs^+$ ions, which enhances the secondary ion yield of electronegative isotopes (Storms et al., 1977), was used to sputter secondary ions from the sample. The primary Cs^+ beam was accelerated to 10 kV and focused with four lenses in a spot of around 50–60 μm diameter. The entry slit was 150 μm, the exit slit was 300 μm, the field aperture was 3000 μm and the energy window was open at 60 eV. The mass resolution power (M/ΔM) was around 5000–6000. Due to implantation of Cs^+ ions and extraction of both negatively charged secondary ions and electrons, the sample surface becomes positively charged. A NEG (Normal incidence Electron Gun) which produced an electronic cloud just in front of the sample is used to compensate the charge on the sample.

Before the measurement the samples were presputtered for 2 min with a scanning beam of 50 μm size and 20 nA. The measurements were performed with a point beam of 50 μm diameter and 5 nA centered in the presputtered region. The secondary ^{12}C-ions were counted with an electron multiplier (counting time 5 s) and the ^{28}Si-ions were measured with a Faraday cup (counting time 3 s), the counting time on the background was 1 s. Counts were corrected for the dead time of the electron multiplier and the background. 20 cycles were measured with a total analysis time of $\sim$8 min.

4. RESULTS

4.1. MIR Spectroscopic Investigation of CO_2

Figure 1a shows IR spectra of selected CO_2 bearing dacitic glasses in comparison to the starting glass synthesized in air. The sharp absorption band at 2348 cm^{-1} is attributed to the ν_3 asymmetric stretching vibration of $CO_{2,mol}$ dissolved in the glass (Fine and Stolper, 1985). This peak is distinct from that for free gaseous molecular CO_2, which would rise to a doublet of unresolved rotational structure centered at $\sim$2350 cm^{-1} (Brooker et al., 1999). The band system at $\sim$1530 cm^{-1} and $\sim$1430 cm^{-1} is attributed to the ν_3 asymmetric stretching vibration of carbonate groups (Blank and Brooker, 1994). Broad features with a maximum intensity at around 1800 cm^{-1} are overtones related to the aluminosilicate framework (Brooker et al., 2001). The band at 1630 cm^{-1} in the spectra of water-rich glasses is assigned to the fundamental bending mode of H_2O molecules.

The concentration of $CO_{2,mol}$ ($C_{CO_{2,mol}}$) in ppm by weight was determined from both the peak height (A_{2348}) and peak area (A^*_{2348}) of the absorption band at 2348 cm^{-1} after subtracting a linear baseline. In the case of peak height the Lambert-Beer law can be written as

$$C_{CO_{2,mol}} = \frac{44.01 \cdot A_{2348}}{\rho \cdot d \cdot \varepsilon_{2348}} \cdot 10^6 \quad (1)$$

where ρ is the density of the glass (g/L), d the thickness of the section (cm) and ε_{2348} is the linear molar absorption coefficient ($L \cdot mol^{-1} \cdot cm^{-1}$) sometimes referred to as the molar absorptivity or the extinction coefficient. The molar absorption coefficients for the molecular CO_2 band in iron-bearing dacitic glasses are not known. In a first approximation, we have evaluated peak areas using an integral molar absorption coefficient of 16700 $\pm$ 1000 $L \cdot mol^{-1} \cdot cm^{-2}$ which was determined for an iron-free dacite-analog composition by Nowak et al. (2003). To quantify $CO_{2,mol}$ from absorbance we have used a linear absorption coefficient of 830 $L \cdot mol^{-1} \cdot cm^{-1}$ which was derived for the same dacite-analog composition from two spectra and carbon speciation data from Nowak et al. (2003, their fig. 1 and table 1).

The quantification of the carbonate in the MIR spectra of dacitic glasses is more difficult because the weak carbonate bands are superimposed by the silicate network bands and by the molecular water band at 1630 cm^{-1}. For basaltic and andesitic glasses a curved baseline fitted to the network bands on both sides of the carbonate doublet is a suitable approach to quantify the intensity of the carbonate bands (Dixon et al., 1995; King and Holloway 2002). In more alumina-rich glasses (such as dacitic glasses) such simple method does not work due to the complexity and intensity of the superimposed band system. Furthermore, the background features change slightly from experiment to experiment because of changing contents of molecular water and variation in oxygen fugacity, which influences iron speciation (although the hydrogen fugacity is approximately constant in the IHPV, the oxygen fugacity in the capsule varies due to different water activities).

As reliable theoretical modeling of the background is not possible, contributions of the superimposed bands only can be removed by subtracting a spectrum of a carbonate-free sample.

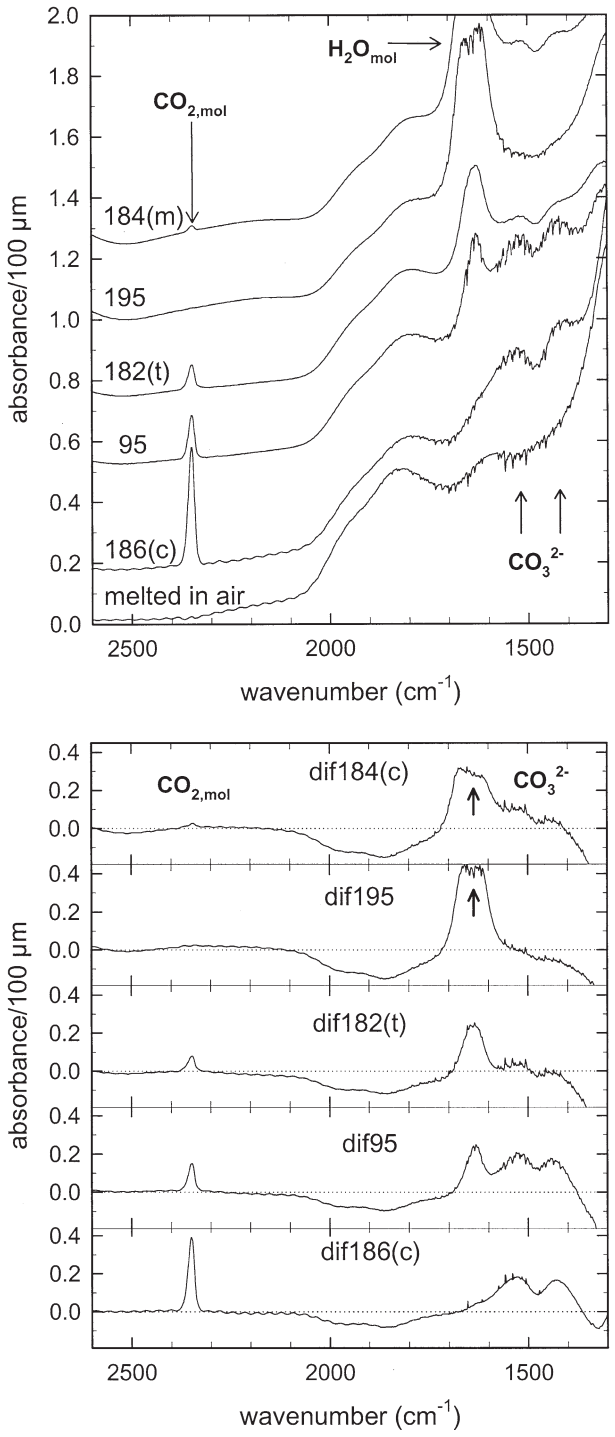

Fig. 1. (a) Midinfrared spectra of dacitic glasses scaled to a thickness of 100 μm. Spectra are plotted with an offset for clarity. The spectrum of a volatile-poor glass synthesized in air is shown for comparison. (b) Difference spectra calculated by subtraction of the spectrum of the air-melted glass from that of H_2O-CO_2 bearing glasses. Water content of the sample increases from bottom to top. Note that the H_2O bending vibration is too strong to be resolved in the two water-rich samples (as indicated by arrows in b).

However, when subtracting the spectrum of the starting glass which is essentially free of CO_2 and H_2O, the contributions of network vibrations can not be eliminated completely (Fig. 1b). The difference spectra show a minimum at ~1870 cm^{-1} which becomes more pronounced with increasing water content, indicating that the intensity of the network vibrations in this spectral range is negatively correlated to the H_2O content of the glasses. This explains also the drop in absorbance on the low-wavenumber side of the carbonate bands. As a consequence, even a semiquantitative evaluation of the carbonate bands is possible only for CO_2-rich and water-poor dacitic glasses when using an air-melted glass as the reference. We have tentatively evaluated the two difference spectra of glasses with the highest CO_2 contents plotted in Figure 1b. The absorbance at 1530 cm^{-1} normalized to 100μm is 0.196 for DC186(c) and 0.152 for DC95 when the absorbance at ~2300 cm^{-1} is chosen as reference. These values of $A_{1530}/100\mu m$ translate to concentrations of CO_2 dissolved as carbonate of 2000 and 1600 ppm, respectively, when using an ε_{1530} value of 170 L · mol^{-1} · cm^{-1}. The value of ε_{1530} is an average determined for the two samples with dacite-analog composition shown in figure 1 of Nowak et al. (2003). For DC186(c) the total CO_2 content determined by IR (considering $C_{CO_{2,mol}}$ from Table 4) agrees within 10% with the value determined by coulometric titration. On the other hand, the deviation between IR data and SIMS measurements is larger (35%) for the more hydrous sample DC95. We conclude that an improvement of the IR spectroscopic determination of carbonate concentrations can be achieved only when using CO_2-free glasses with the same water contents, synthesized and quenched under the same conditions as the CO_2-bearing sample. However, such an approach is extremely expensive and it is not guaranteed that it will work in practice.

4.2. Determination of $CO_{2,total}$ Contents with SIMS

4.2.1. Quality of the Internal Standards

The three glasses prepared as internal SIMS standards are bubble and crystal free. Two sections were prepared from each glass and each section was analyzed by NIR spectroscopy to determine the water content (Table 2). Water was homogeneously distributed in the two samples with low C_{water} (DC182 and DC186) but the water content analyzed by IR is slightly higher than estimated by mass balance (Table 2). The sample with a nominal C_{water} of 5.5 wt% (DC184) is inhomogeneous with respect to dissolved water. We attribute this to the formation of liquid water pools in the pore space of the glass powder before and in the beginning of heating up during the high pressure synthesis. Initially, temperature varies by up to 50°C degree along the capsule (35 mm) and water pools may preferentially be formed in the colder part of the capsule. At run temperature water diffusivity is too slow (Zhang and Behrens, 2000) to equilibrate the batch within synthesis times of several days. CO_2 concentration in the glasses measured by CO_2 titration also was significantly higher than predicted by mass balance of starting materials (Table 2). We attribute these increased volatile contents of the glasses to adsorbed water and CO_2 on the starting materials. Conclusions about CO_2 distribution in the standard glasses are not possible from CO_2 titration (only one analysis per sample) but homogeneity of CO_2 is indicated by the internal consistency of SIMS data during one analytical session (see below). We suppose that the

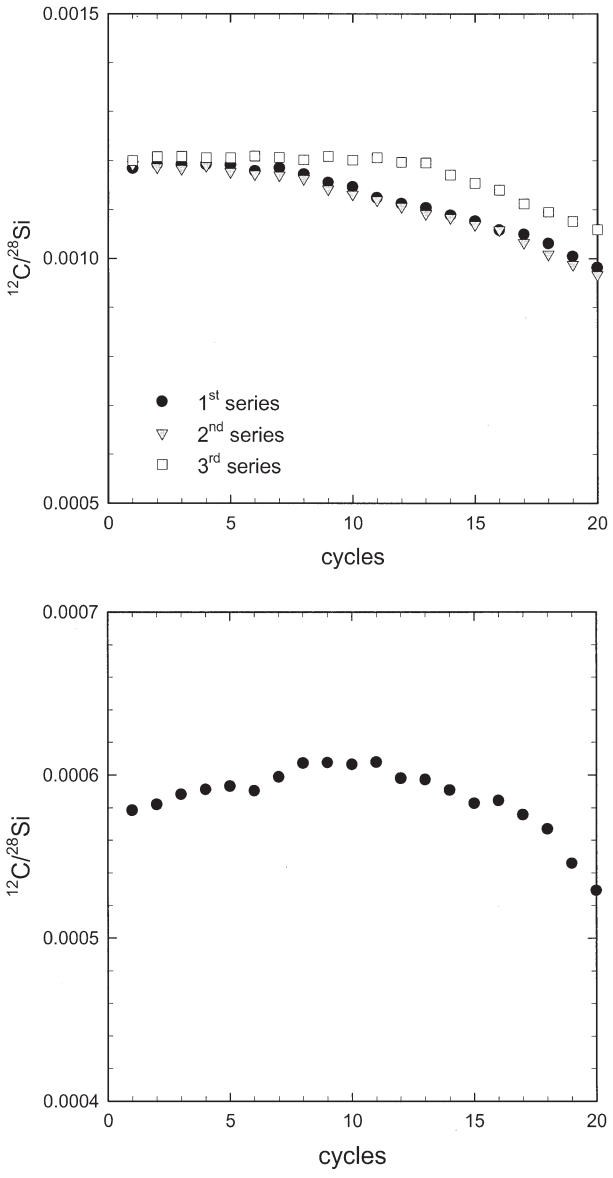

Fig. 2. Typical evolution of the $^{12}C/^{28}Si$ ratio during SIMS measurements. (a) SIMS standard DC186u containing 2565 ppm $CO_{2,total}$ and 0.51 wt% water. The trends measured at different times during one analytical session are representative for glasses with high CO_2 contents (more than 2000 ppm $CO_{2,total}$). (b) Glass obtained after solubility experiment DC197 containing 1376 ppm $CO_{2,total}$ and 1.94 wt% water. The trend is typical for glasses with $CO_{2,total} < 2000$ ppm.

initial temperature gradient on the capsule has only minor influence on CO_2 distribution because CO_2 is in gaseous state already at the beginning of heating, in contrast to H_2O.

4.2.2. *Evolution of the $^{12}C/^{28}Si$ Ratio with Time*

During the measurements on standard and experimental glasses, the $^{12}C/^{28}Si$ ratio (counts of ^{12}C/counts of ^{28}Si) did not remain constant with time. Four different trends were observed:

(1) The $^{12}C/^{28}Si$ ratio continuously decreased with time (Fig. 2a, first and second series).

(2) The $^{12}C/^{28}Si$ ratio remained constant in the first 10–15 cycles before slightly decreasing (Fig. 2a, third series).

(3) The $^{12}C/^{28}Si$ ratio increased for 10–15 cycles and subsequently decreases (Fig. 2b).

(4) In two glasses the $^{12}C/^{28}Si$ ratio firstly increased and remained constant after approximately 15 cycles.

The variation of $^{12}C/^{28}Si$ ratio within one measurement was always below 20% relative. The trends seem to be correlated with the CO_2 content of the glasses. Measurements on glasses with more than 2000 ppm show trends (1) and (2), measurements on glasses with less than 1000 ppm CO_2 showed trends (3) and (4). At intermediate CO_2 contents (1000–2000 ppm) trends (1), (2) and (3) were observed. However, the evolution of $^{12}C/^{28}Si$ with time may not only depend on the CO_2 content but also on other parameters such as synthesis pressure and water content which influence the density of the glass.

The shape of our experimental curves ($^{12}C/^{28}Si$ vs. time) may result from: (1) surface contamination, and/or (2) electromigration of ^{12}C caused by charging (Wilson et al., 1989), and/or (3) a preferential sputtering of ^{12}C from the sample relative to ^{28}Si (Deloule et al., 1995).

(1) Possible contamination of the surface was checked by repolishing the samples with cerium oxide paste after the first tests. The following measurements on the samples did not show significant differences with the former ones, indicating that contamination was a minor problem in our measurements. This is supported by the evolution of the $^{12}C/^{28}Si$ ratio which varies systematically with the CO_2 content of the glasses. In particular the initial increase of the $^{12}C/^{28}Si$ ratio observed for some samples is not expected in the case of surface contamination. We infer that presputtering using an ion beam of relatively high energy was sufficient to remove any carbon contamination from the sample surface.

(2) Charging of the sample surface can result from the poor electrical conductivity of the glasses. The surface charge may initiate a variation of $^{12}C/^{28}Si$ due to charge-driven diffusion of ionized carbon (or hydrogen) to the surface (Note that enrichment or depletion of H_2O also can have an effect on the $^{12}C/^{28}Si$ ratio, because of the changing matrix effect). It is also possible that the secondary-ion beam became unstable due to charge buildup and the intensity dropped because it was partially deflected from the mass spectrometer slits (Hervig et al., 1989).

Sample charging probably can be reduced by using a negative O^- primary beam instead of a Cs^+ beam. Then positive charging due to the emission of secondary electrons can be neutralized by the incoming negative O^- ions. Pan et al. (1991) successfully used an O^- primary beam in their measurements of CO_2 in basaltic glasses. A disadvantage of using a negative ion primary beam is, however, the relatively low sputtering yield of C^- ions. In the study of Pan et al. CO_2 contents were in the range of 7000–15,000 ppm so that this has been a minor problem. However, the amounts of CO_2 in our samples are much smaller (down to a few tens ppm of CO_2). To reduce charging of the surface we used a flood gun as described above.

(3) A preferential sputtering of ^{12}C relative to ^{28}Si would increase the $^{12}C/^{28}Si$ ratio at the beginning of the profile, until the surface layer becomes depleted in ^{12}C (Deloule et al., 1995). This trend could be the result of degassing of CO_2 under vacuum due to heating of the surface by the high energy ion

beam or by electromigration of carbon due to buildup of a surface charge (thus process (3) is not necessarily independent from process (2)). Following this explanation, the continuous decrease of the $^{12}C/^{28}Si$ ratio observed in CO_2-rich glasses indicates a very high mobility of carbon so that the surface of the samples is relatively depleted in ^{12}C already within the 2 min of presputtering. On the other hand, the initial increase of the $^{12}C/^{28}Si$ ratio observed for CO_2-poor glasses suggests a lower mobility of carbon in CO_2-poor glasses so that preferential sputtering of ^{12}C relative to ^{28}Si still is visible in the first measurement cycles.

4.2.3. Calculation of the Ion Yield from Standard Glasses

Considering the different trends of the $^{12}C/^{28}Si$ ratio, we decided to use always the same analytical procedure (2 min presputtering and 20 measurement cycles) and to use the average of the $^{12}C/^{28}Si$ ratios corrected for background to calculate the ion yield and the CO_2 contents in the solubility samples.

The ion yield of ^{12}C relative to ^{28}Si is defined by:

$$\text{ion yield} = \frac{(N_{12_{C^-}}/N_{28_{Si^-}}) \cdot (92.23/98.9)}{C_c/C_{Si}} \quad (2)$$

where $N_{13_{C^-}}$ and $N_{28_{Si^-}}$ are the number of counts on ^{12}C and ^{28}Si measured with the ion probe in standard glasses, 92.23 and 98.9 are the relative abundance of the mass ^{28}Si in natural silicon and ^{12}C in natural carbon, respectively, and C_C and C_{Si} are the concentrations of C and Si in mol per gram of glass measured by independent methods (C by CO_2 titration and Si by electron microprobe).

To define the ion yield as a function of C_{water}, the standard glasses (DC186(b), DC182(t) and DC184(c)) were measured at the beginning of each analytical session. Up to four measurements performed in distances of 1–2 mm agree within analytical error indicating a good homogeneity of the sections. Within one analytical session all measurements on the standard glasses gave consistent ion yields, except for one outlier at the first day (Fig. 3). It can be noted that the ion yield changes from day to day due to changes in measurement conditions so that a calibration is required for each analytical session. A strong matrix effect on the ion yield due to dissolved water is evident from both analytical sessions. The ion yield decreases with the water content of the glass, e.g., a sample with 5 wt% water has a 18–20% lower relative sensitivity factor than a dry sample. To evaluate the SIMS data of glasses from solubility experiments, the relationship between ion yield and water content was determined by linear regressions for each session (first day: *ion yield* = 0.184–0.0067 × wt% H_2O; second day: *ion yield* = 0.207–0.0082 × wt% H_2O).

The total carbon concentration in the sample is calculated by

$$C_c = \frac{(N_{12_{C^-}}/N_{28_{Si^-}}) \cdot (92.23/98.9)}{ion\ yield/C_{Si}} \quad (3)$$

and the concentration of carbon in terms of ppm CO_2 is obtained by

$$C_{CO_{2,total}} = 44.01 \cdot 10^6 \cdot C_c \quad (4)$$

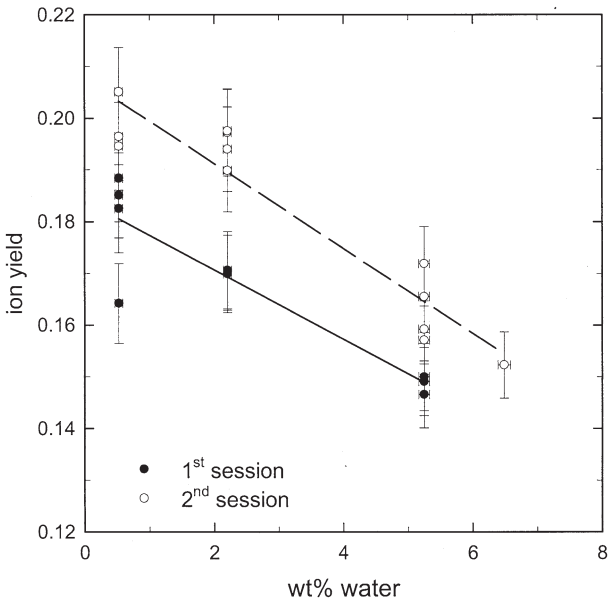

Fig. 3. Ion yield of ^{12}C relative to ^{28}Si as a function of water content for two SIMS sessions.

4.2.4. Reproducibility and Uncertainty of the Carbon Content

The deviation of the CO_2 content in the standard glasses measured by SIMS and by CO_2 titration was up to 4.5% relative, which is close to the error of CO_2 titration (4%), except of the outlier in the first session with a deviation of 9% relative. One or two points with distances between 0.5 and 1.5 mm were analyzed on the experimental glasses (Table 3). The largest deviation between two SIMS analysis on the same glass measured during 1 d was 2.5% relative. On sample DC197 one point was measured in the first analytical session and another one in the second analytical session. The CO_2 contents from both measurements deviate by 5% relative which is within the analytical error. The good agreement of duplicated measurements indicate a high reproducibility in our measurements. Errors in CO_2 content were calculated by error propagation considering the standard errors of the ^{12}C and ^{28}Si intensities, the error in the CO_2 content of the SIMS standard and the standard error of the linear regression of ion yield vs. water content. To account for the different trends of $^{12}C/^{28}Si$ vs. time, we include the largest value for 1 σ standard deviation of ion yield values observed in our measurements (4% relative, in the second series shown in Fig. 2a) as an additional error in the calculation. The resulting overall error in the CO_2 contents of the solubility sample varies from 8 to 15% relative.

4.2.5. CO_2 Solubility in Dacitic Melts

$CO_{2,total}$ varies nonlinearly with $x_{CO_2}^{fluid}$ and it is almost constant in the $x_{CO_2}^{fluid}$ range of 0.8–1 (Table 3, Fig. 4). The maximum CO_2 solubility (corresponding to the solubility of pure CO_2 fluid) is 795 ± 41, 1376 ± 73 and 2949 ± 166 ppm at 100, 200 and 500 MPa, respectively. The variation of the maximum CO_2 solubility in dacitic melts with pressure also appears to be nonlinear, but the number of data points is not

Table 3. Results of CO_2 solubility in dacitic melts at 1250°C.[a]

Sample	P (MPa)	$x_{CO_2}^{fluid}$	f_{CO_2} (bar)	KFT C_{water} (wt%)	SIMS $CO_{2,total}$ (ppm)
DC95	500	0.926	16211	1.57 ± 0.10	2920 ± 436
					2859 ± 427
DC101	500	0.801	14090	3.47 ± 0.11	2949 ± 445
					2949 ± 445
DC102	500	0.565	10756	5.29 ± 0.12	2557 ± 391
					2596 ± 397
DC103	500	0.335	6421	6.80 ± 0.12	2119 ± 335
					2124 ± 335
DC199	200	0.947	3092	0.55 ± 0.11	1317 ± 136
					1319 ± 136
DC198	200	0.927	3028	1.00 ± 0.11	1346 ± 139
					1312 ± 136
DC197	200	0.763	2515	2.05 ± 0.10	1408 ± 147
					1344 ± 141
DC196	200	0.400	1410	3.61 ± 0.10	943 ± 101
					945 ± 101
DC195	200	0.155	604	4.81 ± 0.10	568 ± 61
					564 ± 61
DC156	100	0.825	1045	1.19 ± 0.18	795 ± 66
DC155	100	—		1.44 ± 0.14	698 ± 58
					709 ± 59
DC154	100	0.546	718	2.02 ± 0.11	669 ± 56
DC153	100	0.192	283	3.12 ± 0.11	456 ± 39
DC152	100	—	—	3.64 ± 0.13	320 ± 28

[a] Total water content of glasses was measured using Karl-Fischer titration (KFT) and total carbon dioxide using secondary ion mass spectrometry (SIMS). When two points were analyzed by SIMS, both data are given. f_{CO_2} is calculated after Aranovitch and Newton (1999), using fugacities of pure H_2O and CO_2 from Pitzer and Sterner (1994).

sufficient to resolve properly the pressure dependence (Fig. 5). Tentatively, we have used a second order polynomial to describe the pressure effect at 1250°C: ppm $CO_2 = 7.8240 \cdot P - 0.0039 \cdot P^2$ where P is in MPa.

5. DISCUSSION

5.1. Speciation of CO_2

As shown in Figure 6a, the ratio of $CO_{2,mol}$ (measured by IR spectroscopy) to $CO_{2,total}$ (measured by SIMS) in dacitic glasses strongly decreases with increasing water content. Up to 30% of carbon dioxide is dissolved in molecular form in water-poor glasses but less than 3% in glasses containing more than 3 wt% water (Table 4). This trend is consistent with data of King and Holloway (2002) for andesitic glasses. On the other hand, synthesis pressure and total CO_2 content appears to have a minor influence on CO_2 speciation. The same $CO_{2,mol}/CO_{2,total}$ ratio is observed in dacitic glasses synthesized at different pressures and thus containing different amounts of dissolved CO_2 (Fig. 6b). This observation is consistent with results of previous studies. For instance, Fine and Stolper (1985) found only a minor dependence of the $CO_{2,mol}$/carbonate ratio in sodium aluminosilicate glasses on $CO_{2,total}$ (0–2%), pressure (1.5–3.3 GPa) and temperature of synthesis (1400–1560°C).

It is noteworthy that the variation of carbon speciation in dacitic glasses with C_{water} can not be explained by a dependence of the molar absorption coefficient for the $CO_{2,mol}$ band on water content. Published values of ε_{2348} in aluminosilicate glasses differ by less than a factor of 1.5 (Fine and Stolper, 1985; Blank, 1993; Morizet et al., 2002; Behrens et al., 2004) whereas the $CO_{2,mol}/CO_{2,total}$ ratio in dacitic glasses varies by more than one order of magnitude. Furthermore, it was shown for rhyolitic glasses that water (in the range 0.5 to 7 wt%) does not affect ε_{2348} (Behrens et al., 2004). Additional support for negligible variation of ε_{2348} with water content is given by the constant effective width (19.3 ± 1.3 cm^{-1}, calculated as A^*_{2348}/A_{2348}) and position (2348 ± 1 cm^{-1}) of the molecular CO_2 band.

A crucial point for interpreting the trend in Figure 6a is whether or not the CO_2 speciation measured in glasses at room temperature corresponds to the equilibrium speciation in the melt at the experimental conditions. This question is still discussed controversially. In several studies it was observed that the speciation in CO_2-bearing glasses depends at least to some extent on the run temperature (Stolper et al., 1987; Brooker et al., 1999; Morizet et al., 2002). This is a surprising result because for H_2O speciation it is evident that the equilibrium speciation can not be frozen in from temperatures far above the glass transition (Zhang et al., 1997; Behrens and Nowak, 2003). As outlined by Dingwell and Webb (1990), the exchange frequency of bonds between bridging oxygens and tetrahedral cations is a rate controlling step for both water species reaction and structural relaxation. Thus, the timescale of water species interconversion can not be slower than the timescale for relaxation of the silicate network. However, this may not be the case for carbonate groups which are bound as a bridge between tetrahedral cations. Ab initio calculations of Kubicki and Stolper (1995) have shown that the activation energy for expelling CO_3^{2-} from that silicate network is much higher than that for incorporation of CO_2 into the network. From this result they suggested that the carbonate species present at high tempera-

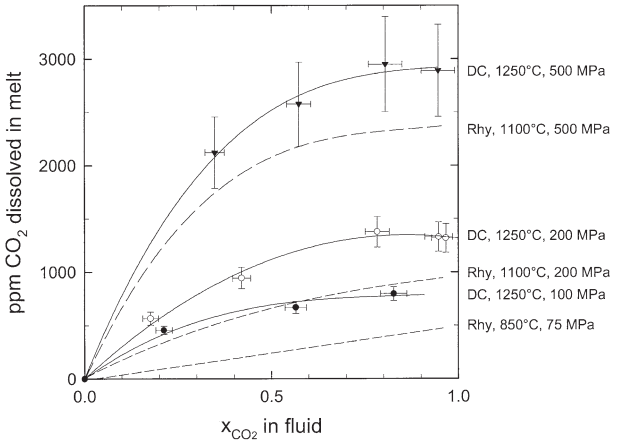

Fig. 4. Total carbon dioxide dissolved in dacitic melts at 1250°C. Solid lines are third order polynomials fitted to the experimental data. Dashed lines are trends for rhyolitic melts at 1100°C, 200 and 500 MPa from Tamic et al. (2001) and at 850°C, 75 MPa from Blank et al. (1993).

ture might be retained metastably during quenching. However, as discussed by Brooker et al. (1999), a much higher energy barrier of 350–400 kJ/mol is required to bring the characteristic timescale of the carbonate reaction into the range of experimental quench so that the high temperature speciation would be fully preserved. They suggested that the speciation measured in the glass at room temperature probably represents an intermediate situation between complete preservation of the high temperature speciation and complete reequilibration during quenching right down T_g. According to Brooker et al. (1999) only a small fraction of carbonate groups probably has

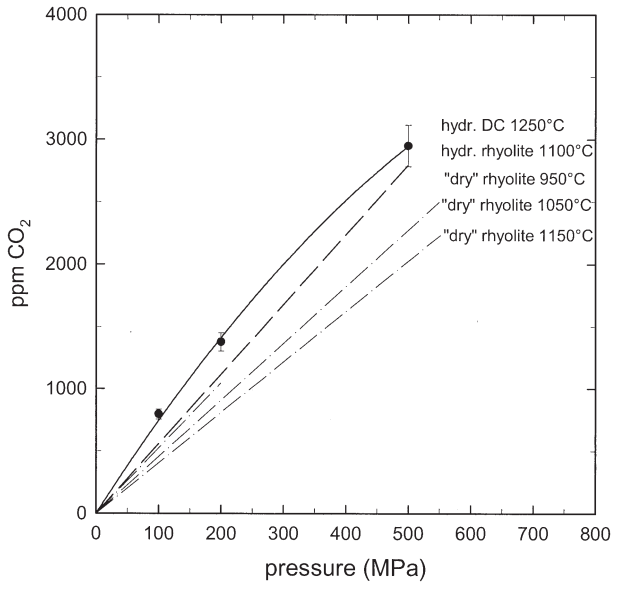

Fig. 5. Pressure dependence of CO_2 solubility in rhyolitic and dacitic melts. The dashed line corresponds to the maximum CO_2 solubility in melts equilibrated with H_2O-CO_2 fluids (Tamic et al., 2001). The dashed-doted lines are for equilibrium with nominally pure CO_2-fluids after Fogel and Rutherford (1990).

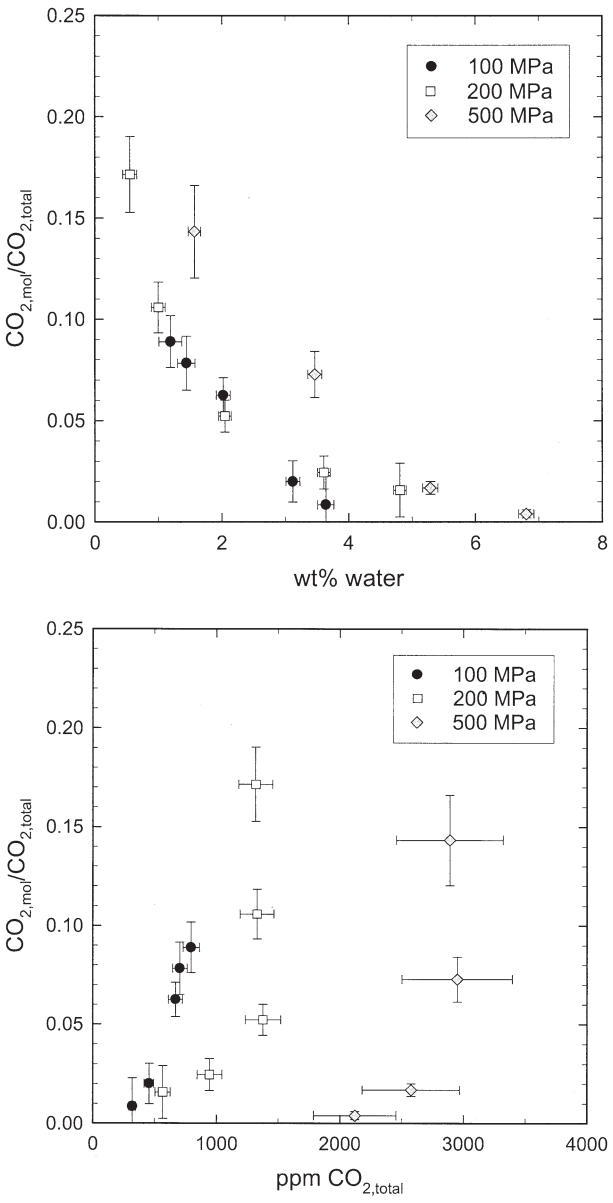

Fig. 6. Variation of the relative abundance of molecular CO_2 in dacitic glasses with (a) total water content of the glasses and (b) total CO_2 content. Data for each pressure are obtained in a single experiment.

a sufficiently slow reaction kinetic to be quenched into the glass. Thus, the major part of carbon species probably is reequilibrated during quench.

Another explanation for the apparent memory on the synthesis conditions might be small differences in water content of the melts as suggested by Nowak et al. (2003). Dissolved water strongly influences the glass transition temperature of alumina-rich melts (Hess and Dingwell, 1996; Richet et al., 1996) and may also selectively stabilize carbon species. The water content of the albitic glasses studied by Stolper et al. (1987) varies from 0.14 to 0.76 wt%. Brooker et al. (1999) estimated the water contents in their glasses along the join $NaAlO_2$-SiO_2 to be at

Table 4. MIR spectroscopy on dacitic glasses.[a]

Sample	Thickness (cm)	A_{2348}	$CO_{2,mol}$ (ppm) from A_{2348}	A^*_{2348} (cm^{-1})	$CO_{2,mol}$ (ppm) from I.I.$_{2348}$
DC186(t)	0.0190	0.548	610 ± 14	11.29	652 ± 15
DC186(c)	0.0190	0.691	770 ± 16	14.40	841 ± 17
DC182(t)	0.0198	0.154	166 ± 11	3.32	185 ± 12
DC182(b)	0.0198	0.259	280 ± 11	5.20	290 ± 12
DC184(c)	0.0195	0.035	39 ± 10	0.70	40 ± 11
DC184(b)	0.0195	0.008	9 ± 9	0.15	9 ± 9
DC95	0.0197	0.282	305 ± 15	5.40	302 ± 12
DC101	0.0192	0.168	187 ± 12	3.12	180 ± 12
DC102	0.0191	0.044	50 ± 11	0.76	44 ± 12
DC103	0.0189	0.010	11 ± 11	0.13	8 ± 8
DC199	0.0144	0.154	226 ± 15	2.95	224 ± 16
DC198	0.0134	0.089	141 ± 16	1.79	147 ± 17
DC197	0.0142	0.048	72 ± 15	0.87	67 ± 15
DC196	0.0148	0.016	23 ± 15	0.41	31 ± 15
DC195	0.0145	0.006	9 ± 9	0.26	20 ± 15
DC156	0.0129	0.043	71 ± 17	0.77	65 ± 17
DC155	0.0131	0.034	55 ± 16	0.61	51 ± 17
DC154	0.0234	0.046	42 ± 9	0.84	40 ± 10
DC153	0.0234	0.010	9 ± 9	0.20	10 ± 9
DC152	0.0234	0.003	3 ± 3	0.04	2 ± 2

[a] A_{2348} and A^*_{2348} are the peak height and peak area, respectively, of the band at 2348 cm^{-1} in IR absorption spectra. Errors in $CO_{2,mol}$ concentration are based only on the uncertainties in density, thickness and absorbance but do not consider the (unknown) uncertainty in using molar absorption coefficients derived for an iron-free dacite-analog composition (Nowak et al., 2003).

0.30 ± 0.05 wt% but no details are given. Morizet et al. (2002) do not report H_2O contents of their haplo-phonolitic glasses.

On the other hand, annealing experiments indicate that carbon speciation in CO_2-bearing glasses may be readjusted rapidly even below the glass transition (Morizet et al., 2001; Nowak et al., 2003). The studies consistently show that the relative abundance of molecular CO_2 in jadeitic, albitic and iron-free dacitic glasses increases with temperature which contrasts to earlier suggestions based on glasses quenched from high temperature (Stolper et al., 1987). The timescale for the CO_2 species reaction ($CO_2 + O^{2-} = CO_3^{2-}$) was found to be below 100 min in iron-free dacitic glasses at 500°C (Nowak et al., 2003) and below 500 min in jadeitic glasses at 400°C (Morizet et al., 2002). The relatively fast reaction implies that the CO_2 species reaction may be decoupled from the structural relaxation of the melt and a (metastable) species equilibrium can be achieved several tenth to hundred degrees below the glass transition temperature T_g within several hours or days. However, when using a rapid quench as in our study, the experimental timescale ($\sim 10^{-2}$ s) seems to be too short to readjust CO_2 species concentrations significantly below T_g. Therefore, we assume that species concentration in our glasses basically reflects the equilibrium speciation near the glass transition. Since an increasing water content lowers the viscosity and thus lowers the fictive temperature, the observed trend for CO_2 speciation in dacitic glasses may simply reflect the variation in T_g. To test this hypothesis, we estimated the glass transition temperature of the dacitic melts as a function of water content. According to Scherer (1984) at a cooling rate of 150 K/s, T_g corresponds to the temperature at which the melt viscosity equals $10^{9.12}$ Pa · s. Using the viscosity models for rhyolitic melts (Hess and Dingwell, 1996) and iron-free andesitic melts (Richet et al., 1996) T_g can be bracketed for our hydrous dacitic melts. The calculated T_g values for a melt containing 4 wt% H_2O varies from 516°C (rhyolite) to 543°C (andesite). According to Nowak et al. (2003), the $CO_{2,mol}/CO_{2,total}$ ratio in dry iron-free dacitic glasses is 0.361 and 0.395, respectively, at these temperatures. Both values are significantly higher than the measured ratio of <0.03 (Fig. 6a). It is unlikely that the small difference in bulk composition of the dacites used in our study and in the study of Nowak et al. (2003) accounts for the large difference between experimental and calculated $CO_{2,mol}/CO_{2,total}$ values. Thus we conclude that the low $CO_{2,mol}/CO_{2,total}$ ratios in the water-rich melts are due to a stabilization of carbonate by hydrous species or by a modification of the glass structure induced by dissolved water. This explanation is supported by data of Kohn et al. (1991) who measured the CO_2 speciation in a hydrous and an anhydrous albite glass by NMR spectroscopy. In the hydrous albite glass with 6 wt% water the overall carbonate to $CO_{2,mol}$ ratio is much larger than in the anhydrous glass.

5.2. CO_2 Solubility

5.2.1. Effect of Melt Composition on CO_2 Solubility

The maximum CO_2 solubility in dacitic melts equilibrated with H_2O-CO_2 fluids is comparable to data for rhyolitic to basaltic melts (Fogel and Rutherford, 1990; Mattey, 1991; Pan et al., 1991; Dixon et al., 1995; Tamic et al., 2001; King et al. 2002). The experimental data indicate that the solubility of CO_2 varies only weakly with melt composition in this compositional range. A more detailed analysis of the effect of melt composition on CO_2 solubility in rhyolitic to basaltic melts is not possible due to discrepancies between the data sets. For instance, Mattey (1991) reported a much lower CO_2 solubility of 0.45–0.51 wt% in a MORB basalt at 1.0 GPa and 1200–1400°C than found by Pan et al. (1991) in a tholeiitic basalt at

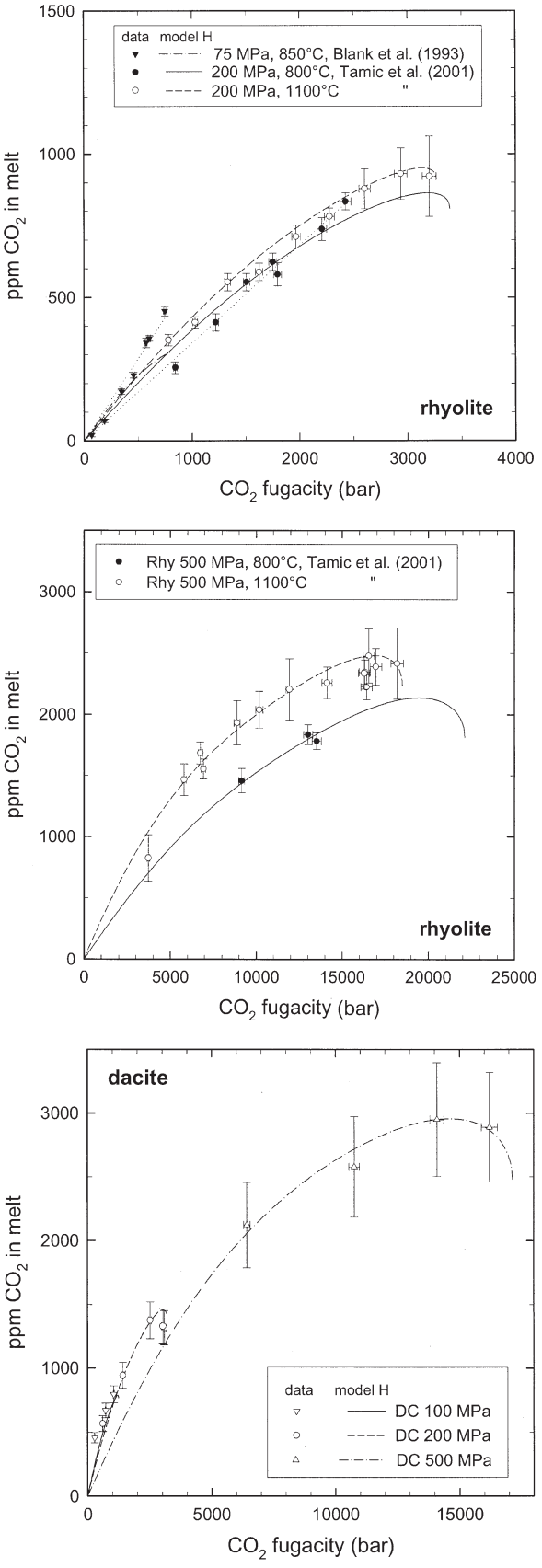

Fig. 7. Dependence of the total CO_2 content dissolved in the melt on the CO_2 fugacity for (a) rhyolitic melts at 75 and 200 MPa, (b) rhyolitic melts at 500 MPa and (c) dacitic melts at 1250°C and various pressures. Dotted lines indicate Henrian behavior for rhyolite at 75 MPa, 850°C and 200 MPa, 800°C. Other lines are fits using the models for hydrous melts. The strong decrease in CO_2 solubility predicted by the model for high CO_2 fugacity is attributed to the promoting effect of dissolved H_2O on CO_2 solubility.

1.0 GPa and 1300–1500°C (0.77 wt%). Furthermore, the value of 0.3 wt% given for CO_2 solubility in an intermediate (andesitic) melt at 1300°C and 1.0 GPa (King and Holloway, 2002) appears to be relatively low compared to data for basalt (Mattey, 1991; Pan et al., 1991) and extrapolated data for rhyolite (Fogel and Rutherford, 1990). The discrepancy in the data is probably due to experimental and analytical difficulties, i.e., in the control and analysis of the fluid composition and in the calibration of the analytical method for CO_2 quantification in glasses.

In both rhyolitic and basaltic melts equilibrated with H_2O-CO_2 fluids a Henrian behavior was observed at pressures below 100 MPa (Blank et al., 1993; Dixon et al., 1995). Data of Tamic et al. (2001) for CO_2-solubility in rhyolitic melts at 800°C, 200 MPa are also consistent with a Henrian behavior (Fig. 7a), but at higher pressure or higher temperature deviations from simple proportionality between f_{CO_2} and $C_{CO_{2,total}}$ is evident (Figs. 7a,b). Our results for dacitic melts at 1250°C and pressures of 100–500 MPa show also a nonlinear variation of the total CO_2 concentration in the melt with CO_2 fugacity (Fig. 7c). A strong increase of CO_2 solubility with water content of the melt was found also for andesitic melts equilibrated with C-H-O fluids at 1.0 GPa and 1300°C (King and Holloway, 2002). A possible interpretation of these trends is that at least at high temperatures and pressures CO_2 solubility is strongly enhanced by dissolved H_2O.

5.2.2. *Thermodynamic Treatment*

Dissolution of CO_2 in silicate melt can be treated as a two-step process, a heterogeneous reaction of the fluid with the melt and a homogeneous reaction between carbon species in the melt (Holloway and Blank, 1994). The heterogeneous reaction can be expressed as:

$$CO_2^{fluid} \leftrightarrow CO_{2,mol}^{melt} \tag{5}$$

Assuming ideal mixing of CO_2 molecules, carbonate groups and oxygen atoms and hydrons species, the equilibrium constant K_1

$$K_1 = \frac{x_{CO_{2,mol}}^{melt}}{f_{CO_2}}, \tag{6}$$

The mole fraction of molecular CO_2, $x_{CO_{2,mol}}^{melt}$, is defined as

$$x_{CO_{2,mol}}^{melt} = \frac{n_{CO_{2,mol}}^{melt}}{n_{CO_{2,mol}}^{melt} + n_{CO_3^{2-}}^{melt} + n_{water}^{melt} + n_{O^{2-}}^{melt}}, \tag{7}$$

where n_i is the number of moles of the $CO_{2,mol}$, carbonate, water or oxygen per unit mass of sample. Choosing for instance

a unit mass of 100 g, the mole number of oxygen corresponds to (100-wt% H_2O-wt% CO_2)/(molecular weight of the anhydrous glass calculated on one-oxygen basis). In Eqn. 6 we do not distinguish hydrous species (OH and H_2O). The main reason for doing so is that otherwise the number of variables becomes too large to constrain a thermodynamic model by the experimental data. It is noteworthy that the value of $x^{melt}_{CO_{2,mol}}$ does not change when hydrous species are considered in the calculation because the increase of hydrous species is compensated by a decrease in $O^{2-,melt}$ according to the reaction $H_2O^{melt} + O^{2-,melt} = 2\ OH^{melt}$. Provided that the molecular CO_2 solubility obeys Henry's law ($x^{melt}_{CO_{2,total}}$ is proportional to f_{CO_2}), K_1 can be written as

$$K_1 = K_1^o \cdot \exp\left(\frac{-V^{melt}_{CO_{2,mol}}(P - P_{ref})}{RT} - \frac{\Delta H^o_{CO_{2,mol}}}{R}\left(\frac{1}{T} - \frac{1}{T_{ref}}\right)\right) \tag{8}$$

where K_1° is the equilibrium constant at a reference temperature T_{ref} and reference pressure P_{ref}, $V^{melt}_{CO_{2,melt}}$ is the molar volume of CO_2 molecules in the melt and $\Delta H^\circ_{CO_{2,mol}}$ is the enthalpy for reaction 5.

The homogeneous speciation reaction in the melt can be expressed as

$$CO^{melt}_{2,mol} + O^{2-,melt}_r \leftrightarrow CO^{2-,melt}_3, \tag{9}$$

with the equlibrium constant

$$K_2 = \frac{x^{melt}_{CO_3^{2-}}}{x^{melt}_{CO_{2,mol}} \cdot x^{melt}_{O_r^{2-}}} \tag{10}$$

$x^{melt}_{CO_3^{2-}}$ is defined analog to $x^{melt}_{CO_{2,mol}}$ and $x^{melt}_{O_r^{2-}}$ denotes to the mole fraction of reactive oxygen in the melt. Usually all oxygens in the melt are assumed to be indistinguishable and equally available for the reaction with $CO_{2,mol}$ (e.g., Stolper et al., 1987; Holloway and Blank, 1994). The pressure and temperature dependence of K_2 can be expressed as

$$K_2 = K_2^o \cdot \exp\left(\frac{-\Delta V^o(P - P_{ref})}{RT} - \frac{\Delta H^o}{R}\left(\frac{1}{T} - \frac{1}{T_{ref}}\right)\right) \tag{11}$$

where ΔV° is the reaction volume and ΔH° is the reaction enthalpy of reaction 9. The total CO_2 content in the melt is

$$x^{melt}_{CO_{2,total}} = x^{melt}_{CO_{2,mol}} + x^{melt}_{CO_3^{2-}} \tag{12}$$

$$x^{melt}_{CO_{2,total}} = (1 + K_2 \cdot x^{melt}_{O_r^{2-}}) \cdot K_1 \cdot f_{CO_2} \tag{13}$$

If K_2 is negligible ($CO_{2,mol}$ is the dominant carbon species as in rhyolitic melts), Eqn. 13 simplifies to

$$x^{melt}_{CO_{2,total}} = K_1 \cdot f_{CO_2} \tag{14}$$

On the other hand, if $CO_{2,mol}$ is negligible as in tholeitic, basanitic and leucitic melts, the total carbon content is calculated as

$$x^{melt}_{CO_{2,total}} = x^{melt}_{O_r^{2-}} \cdot K_1 \cdot K_2 \cdot f_{CO_2} \tag{15}$$

5.2.3. Modeling Hydrous Melts

The approach outlined in the previous section accurately describes the CO_2 solubility behavior in nominally dry melts and in melts equilibrated with H_2O-CO_2 fluids at pressures $<$100 MPa (Holloway and Blank, 1994; Dixon et al. 1995). At these conditions the CO_2 solubility obeys Henry's law. Hydrous rhyolitic and dacitic melts, however, show clearly a nonlinear variation of $x^{melt}_{CO_{2,total}}$ with CO_2 fugacity (Figs. 7a,b) which indicates an enhancement of CO_2 solubility by dissolved water. Possible explanations for this behavior are (i) either that OH groups formed by dissolution of H_2O increase the number of reactive oxygens in the melt and (ii) or that one or both of the equilibrium constants K_1 and K_2 depend on water content of the melt. Explanation (i) suggests that carbonate becomes increasingly more abundant with increasing water content which is consistent with speciation data for dacitic glasses. However, IR spectra yield no evidence for any carbonate in hydrous rhyolitic glasses (Tamic et al., 2001). A weak, unresolved carbonate doublet may be present in the spectra and the absorption coefficient for the carbonate band system in rhyolitic glasses is probably low (Brooker et al., 1999) found decreasing absorption coefficients for $CO_{2,mol}$ and carbonate bands with increasing polymerization in glasses along the $NaAlO_2$-SiO_2 join). Hence, it can not be excluded that a minor portion of $CO_{2,total}$ is bond as carbonate in rhyolitic glasses. However, at the high temperatures of the solubility experiments the concentration of carbonate is expected to be negligible due to the progradely increasing abundance of $CO_{2,mol}$ (Morizet et al., 2001; Nowak et al., 2003). Hence, we conclude that dissolved H_2O increases K_1 in silicic melts or in other words CO_2 molecules are stabilized in the melt by hydrous species. K_2 may be also affected by hydrous species but we can not constrain this in our thermodynamic model due to the absence of CO_2 speciation data for hydrous melts. The functional relationship between water content of the melt and K_1 is not known from theory. As a simple approach we have chosen a log-linear relationship

$$K_1^o = K_1^{o,d} \cdot \exp\,(k \cdot x^{melt}_{water}) \tag{16}$$

where $K_1^{o,d}$ is the equilibrium constant for the dry melt at T_{ref} and P_{ref}, x^{melt}_{water} is the mol fraction of H_2O dissolved in the melt, and k a constant. It is noteworthy that the exponential variation of K_1 corresponds to a linear change in free energy with composition. Combining Eqn. 7, 12 and 15 gives

$$x^{melt}_{CO_{2,total}} = (1 + K_2 \cdot x^{melt}_{O_r^{2-}}) \cdot f_{CO_2} \cdot K_1^{o,d} \times \exp\left(k \cdot x_{water} - \frac{V^{melt}_{CO_{2,mol}}(P - P_{ref})}{RT} - \frac{\Delta H^o_{CO_{2,mol}}}{R}\left(\frac{1}{T} - \frac{1}{T_{ref}}\right)\right) \tag{17}$$

To test the thermodynamic model we have firstly analyzed data for rhyolitic melts which dominantly or exclusively incorporate molecular CO_2. In the next step we will deal with dacitic melts which contain both $CO_{2,mol}$ and carbonate.

5.2.4. CO_2 Solubility in Rhyolitic Melts

Experimental data on CO_2 solubility in rhyolitic melts are summarized in Table 5. Fogel and Rutherford (1990) studied

Table 5. Data used in thermodynamic modeling of CO_2 solubility in rhyolitic melts and predictions of the solubility models.[a]

	P (MPa)	T (K)	$x_{CO_2}^{fluid}$	f_{CO_2} (bar)	C_{water} (wt%)	x_{water}	$CO_{2,mol}$ (ppm)	$x_{CO_{2,total}}^{melt}$ ($\cong 10^4$)	$x_{CO_{2,total}}^{melt}$ ($\cong 10^4$) predicted by model H
					Tamic et al. (2001)				
Ech1	200	1073	0.692	2427	2.93	0.0517	834	6.02	5.59
Ech7	200	1073	0.625	2208	3.20	0.0563	738	5.31	5.22
Ech6	200	1073	0.498	1796	3.81	0.0667	580	4.15	4.48
Ech2	200	1073	0.484	1751	3.94	0.0689	623	4.47	4.42
Ech8	200	1073	0.409	1507	4.13	0.0721	553	3.96	3.86
Ech9	200	1073	0.322	1221	4.61	0.0802	413	2.94	3.27
Ech10	200	1073	0.212	845	5.02	0.0871	255	1.81	2.34
Ech66	200	1373	0.959	3203	0.54	0.0097	922	6.79	6.94
Ech65	200	1373	0.878	2938	1.41	0.0252	931	6.81	6.89
Ech64	200	1373	0.774	2605	2.05	0.0364	878	6.38	6.47
Ech63	200	1373	0.670	2278	2.46	0.0435	781	5.66	5.88
Ech62	200	1373	0.570	1967	2.85	0.0503	711	5.14	5.26
Ech17	200	1373	0.460	1625	3.53	0.0620	588	4.22	4.62
Ech18	200	1373	0.367	1332	3.87	0.0677	553	3.97	3.90
Ech19	200	1373	0.274	1030	4.37	0.0762	413	2.95	3.14
Ech20	200	1373	0.201	781	4.67	0.0812	351	2.54	2.45
Ech37	500	1073	0.572	13521	5.18	0.0898	1783	12.65	13.08
Ech38	500	1073	0.547	13020	5.32	0.0921	1835	13.01	12.76
Ech39	500	1073	0.354	9156	6.49	0.1113	1458	10.24	9.91
Ech75	500	1373	0.963	18191	0.50	0.0089	2415	17.78	17.06
Ech74	500	1373	0.896	16959	1.14	0.0204	2388	17.50	16.88
Ech73	500	1373	0.873	16544	1.35	0.0241	2476	18.11	16.78
Ech72	500	1373	0.866	16418	1.82	0.0324	2222	16.19	17.39
Ech59	500	1373	0.860	16310	2.45	0.0434	2344	17.00	18.28
Ech71	500	1373	0.858	16274	2.18	0.0387	2336	16.97	17.81
Ech58	500	1373	0.735	14118	3.29	0.0579	2257	16.25	16.98
Ech57	500	1373	0.606	11937	3.91	0.0684	2204	15.80	15.24
Ech22	500	1373	0.500	10178	5.09	0.0883	2037	14.47	14.41
Ech56	500	1373	0.422	8882	5.21	0.0903	1932	13.71	12.71
Ech61	500	1373	0.308	6929	6.53	0.1120	1554	10.91	11.10
Ech24	500	1373	0.298	6751	6.70	0.1147	1686	11.83	10.97
Ech41	500	1373	0.246	5802	7.04	0.1203	1466	10.26	9.70
Ech36	500	1373	0.143	3731	8.19	0.1387	825	5.73	6.86
					Blank et al. (1993)				
2	75	1123	0.680	574	1.88	0.0334	342	2.48	1.90
3	75	1123	0.520	457	2.24	0.0397	228	1.66	1.55
4	75	1123	0.060	69	3.34	0.0587	20	0.15	0.25
5	75	1123	0.180	187	3.23	0.0568	70	0.51	0.70
7	75	1123	0.370	344	2.28	0.0404	172	1.25	1.19
9	75	1123	0.910	749	0.51	0.0092	452	3.33	2.19
10	75	1123	0.720	603	1.35	0.0241	357	2.61	1.91
					Fogel and Rutherford (1990)				
134	101	1223		1308	0.14	0.0025	465	3.43	3.47
152	151	1223		2238	0.11	0.0020	739	5.46	5.07
130	199.3	1223		3429	0.26	0.0047	1115	8.23	6.77
111	50.4	1323		564	0.11	0.0020	147	1.08	1.76
123	100	1323		1275	0.13	0.0023	382	2.82	3.47
124	150	1323		2206	0.11	0.0020	621	4.58	5.19
108	202.5	1323		3479	0.14	0.0024	950	7.02	7.05
142	204	1323		3520	0.07	0.0013	911	6.69	7.49
128	249	1323		4920	0.19	0.0033	1204	8.89	8.75
139	352.9	1323		9472	0.22	0.0040	1568	11.58	12.55
153	432.4	1323		14650	0.19	0.0034	2029	14.99	15.38
153C	432.4	1323		14650	0.18	0.0033	2232	16.49	15.38
136	202.9	1423		3441	0.07	0.0012	875	6.47	7.21
149	348.7	1423		8929	0.11	0.0019	1394	10.29	12.79
					data from Fogel and Rutherford (1993) not used in fitting				
145	549.6	1323		26070	0.24	0.0043	2261	16.70	19.62
148	661.2	1323		43006	0.31	0.0056	2889	21.32	23.63
131	450	1423		15251	0.10	0.0018	1819	13.44	16.54
147	551.4	1423		24588	0.19	0.0035	2226	16.44	20.49

[a] Fugacities of pure CO_2 fluids were calculated after Pitzer and Sterner (1994). Activity coefficients for mixed H_2O-CO_2 fluids were calculated after Aranovich and Newton (1999). All CO_2 solubility data are based on IR spectroscopy. Data were recalculated using $\varepsilon_{2348} = 1214\ L \cdot mol^{-1} \cdot cm^{-1}$ (Behrens et al., 2004).

Table 6. Model parameters for CO_2 solubility in rhyolitic and dacitic melts.[a]

	Rhyolite					Dacite
	H&B94	Model D	Model D′	Model H	Model H′	Model H[b]
input data		water-poor melts	dry and hydrous melts	hydrous melts	dry and hydrous melts	hydrous melts
Data source	F&R90, B93	F&R90, B93	F&R90, B93, T01	B93, T01	F&R90, B93, T01	this study
samples	unknown	21	54	40	54	12
ln K_1^o	–14.44 (±0.06)	–14.74 (±0.05)	–14.71 (±0.08)	–14.84 (±0.05)*	–14.76 (±0.04)*	–14.37 (±0.08)*
ΔH^o (kJ/mol)	–27.1 (±1.0)	–25.1 (±3.7)	–9.4 (±2.7)	0[a]	–2.5 (±1.4)	0
ΔV^o (cm^3/mol)	28.1 (±0.8)	28.1 (±1.5)	26.3 (±2.0)	31.7 (±1.2)	32.1 (±1.2)	46.5 (±2.7)
k	—	—	—	5.20 (±0.31)	4.44 (±0.36)	5.83 (±0.81)
P_{ref} (MPa)	0.1	0.1	0.1	0.1	0.1	0.1
T_{ref} (°C)	850	1000	1000	1000	1000	1250
standard error of estimate of $X_{CO2,total}$ ($\times 10^4$)	not given	0.60	1.71	0.72	0.91	1.07
r^2	not given	0.9911	0.9301	0.9891	0.9805	0.9798

Notes. Numbers in parentheses are 1σ errors of the parameters derived from the regression.

[a] ΔH^o obtained by fitting was statistically not significant (−0.5 (± 1.3) kJ/mol) and, hence, it was set to 0 for model H.

[b] K_2 was calculated using the speciation data of Nowak et al. (2003) for an iron-free dacitic composition (ln $K_2 = -1.559 + 3488/1$).

* ln $K_1^{o,d}$ is given. Column H&B94 refers to the parameters derived by Holloway and Blank (1994) from CO_2 solubility data of Blank et al. (1993). Note that these authors have calculated fugacities at pressures up to 400 MPa using the modified Redlich-Kwong equation of Holloway (1987) and at higher pressure using the corresponding equation of state of Saxena and Fei (1987). F&R90 = Fogel and Rutherford (1990), B93 = Blank et al. (1993), T01 = Tamic et al. (2001).

melts equilibrated with essentially pure CO_2 at temperatures 950, 1050 and 1150°C and pressures from 66 to 660 MPa. Blank et al. (1993) measured CO_2 solubility in rhyolitic melts in equilibrium with H_2O-CO_2 fluids at 850°C and 75 MPa. Similar experiments were performed by Tamic et al. (2001) at 800 and 1100°C and 200 and 500 MPa. In all studies CO_2 concentration in the glasses was measured by IR spectroscopy using the band at 2348 cm^{-1}. Data of Fogel and Rutherford (1990) are based on the absorption coefficient ε_{2348} of 945 L · mol^{-1} · cm^{-1} determined by Fine and Stolper (1985) for sodium aluminosilicate glasses whereas Blank et al. (1993) and Tamic et al. (2001) have used the ε_{2348} value of 1066 L · mol^{-1} · cm^{-1} determined for rhyolitic glasses by Blank (1993). For internal consistency the CO_2 contents of all studies were recalculated on the basis of the ε_{2348} value of 1214 L · mol^{-1} · cm^{-1} determined by Behrens et al. (2004).

For simplicity we assume that the fluids are composed only by H_2O and CO_2. After Churakov (personal communication, based on the equations of state published in Churakov and Gottschalk, 2003) CO is negligible under the relatively oxidizing conditions in hydrous systems studied by Blank et al. (1993) and Tamic et al. (2001). On the other hand, up to 30 mol% CO might have been present in the water-poor fluids of Fogel and Rutherford (1990). The effect of this dissolved silicate material in the fluid on activities in the CO_2-H_2O system is perhaps quite significant, but completely unknown. Hence, we can not account for it in our modeling. Fugacities of pure fluids were computed uniquely after Pitzer and Sterner (1994). Activity coefficients of H_2O and CO_2 in binary H_2O-CO_2 fluids were calculated after Aranovich and Newton (1999) using molar volumes of pure H_2O and CO_2 from Pitzer and Sterner (1994). Note that a different computation method for fugacities was used by Holloway and Blank (1994).

To compare our approach to their thermodynamic modeling, we have refitted the data of Fogel and Rutherford (1990) and Blank et al. (1993) using the model *D* (Eqn. 17, $K_2 = 0$, $k = 0$, *D* refers to "dry" melts). Samples of Fogel and Rutherford which were largely crystallized or which yield absorbances of the IR band at 2348 cm^{-1} larger than 2 were not considered in the fit. Parameters derived from our fitting are in good agreement with those obtained by Holloway and Blank (1994) (Table 6). The difference in lnK_1 is due mainly to the use of different ε_{2348} values (factor of 1066/1214 in CO_2 solubility). However, it has to be noted that CO_2 solubility in most hydrous rhyolitic melts from Blank et al. (1993) (their samples 3, 4, 5 and 7) is systematically overestimated by the fit. Applying model *D* to melts equilibrated with H_2O-CO_2 fluids at 200 and 500 MPa (Tamic et al., 2001) systematically underestimates the CO_2 solubility by up to a factor of 1.8. The discrepancy is especially large at low f_{CO_2}. Including the data of Tamic et al. (2001) in the fit does not improve the predictions for hydrous melts (Model *D*′). There is still a large discrepancy to the experimental data of Tamic et al. at low f_{CO_2} (up to a factor of 1.7). The model *H* (Eqn. 17, $K_2 = 0$, $k > 0$, *H* refers to hydrous melts) is based on data of Blank et al. (1993) and Tamic et al. (2001). This model reproduces all data of Tamic et al. within 8% relative except of two outliers at low $x_{CO_2}^{fluid}$ (Table 5). The linear trend in the data of Blank et al. (1993), however, is not reproduced. At 75 MPa and 850°C the model *H* underestimates the CO_2 solubility in rhyolitic melts at $x_{CO_2}^{fluid} < 0.4$ but it overestimates the CO_2 solubility at higher $x_{CO_2}^{fluid}$. Data of Fogel and Rutherford (1990) for water-poor melts are reproduced within 20% relative except of one experiment (the one with lowest CO_2 content, Table 4). This agreement is relatively good considering the large decrease in CO_2 solubility towards dry melts predicted by the model and considering that the fluid composition was not analyzed in that study. Including the data of Fogel and Rutherford in the model (Model *H*′) decreases the fit quality (Table 6). We prefer model *H* to model *H*′ for

hydrous rhyolitic melts because of the uncertainty in the fluid composition in the study of Fogel and Rutherford.

The partial molar volume of CO_2 in hydrous rhyolitic melts (31.7 ± 1.2 cm^3/mol) is in good agreement with the value found for water-poor melts (28.1 ± 1.5 cm^3/mol). Our model for the hydrous melt indicates that the dissolution enthalpy for CO_2 is negligible. This contrasts to the $\Delta H°$ value of −27.1 kJ/mol found for water-poor rhyolitic melts (Holloway and Blank, 1994). However, it should be noted that the value for water-poor melts is based mainly on the data of Fogel and Rutherford (1990) for which the fluid composition is unknown. The decrease in CO_2 solubility with increasing temperature observed in that study can be simply due to an increasing abundance of CO (see fig. 6 of Fogel and Rutherford, 1990).

The reproduction of the experimental data for CO_2 solubility in rhyolitic melts by our new thermodynamic model (*H*) is similar to the purely empirical calculation model of Liu et al. (2004). The model of Liu et al. (2004) has the advantage of an easier calculation procedure. However, an extrapolation to other P-T conditions then used in the experiments is more uncertain in the empirical approach.

5.2.5. CO_2 Solubility in Dacitic Melts

Data for dacitic melts were fitted by Eqn. 17 using the equilibrium constant for the CO_2 speciation reaction ($\ln K_2 = -3.849 + 3488/T$) of Nowak et al. (2003). It is noteworthy that this can be only a first approach because (i) K_2 was measured nearby and below the glass transition (500–700°C) and, hence, a large extrapolation towards higher temperature is required and (ii) the dependence of CO_2 speciation on water content has not been determined.

The agreement between predicted and measured CO_2 solubility is very good at high pressure and high $x_{CO_2}^{fluid}$ (less than 10% deviation). At low $x_{CO_2}^{fluid}$ and low pressure the predicted CO_2 solubility is lower than the measured values (by 21% at 200 MPa, $x_{CO_2}^{fluid} = 0.16$ and by 45% at 100 MPa, $x_{CO_2}^{fluid} = 0.19$). This suggests that our model for hydrous melts can not be extrapolated towards lower pressure (note also the deviation of the 75 MPa data from Blank et al., 1993, to the model for hydrous rhyolite). The partial molar volume of CO_2 of 46.5 ± 2.7 cm^3/mol calculated by model *H* for hydrous dacitic melts is significantly larger than for other melt compositions (21.7–28.1 cm^3/mol for ryholtic, tholeiitic, basanitic and leucitic melts; Holloway and Blank, 1994). In other words this means that the pressure dependence of CO_2-solubility is more pronounced for dacitic melts.

6. CONCLUSIONS

New CO_2 solubility data are presented for dacitic melts equilibrated with H_2O-CO_2 fluids at 1250°C and pressures of 100, 200 and 500 MPa. SIMS was calibrated to quantify the total carbon content of the quenched glasses using self-made glass standards. The relative sensitivity factor for $^{12}C/^{28}Si$ was found to decrease systematically with water content of the glasses. Due to variations in SIMS measurement conditions calibration lines have to be determined for each analytical session.

A strong nonlinear correlation between CO_2 solubility and $x_{CO_2}^{fluid}$ was found for dacitic melts similar to previous findings for rhyolitic melts (Tamic et al., 2001). The trend indicates a non-Henrian behavior of CO_2 solubility in equilibrium with H_2O-CO_2 fluids. Our interpretation of this result is that dissolved H_2O strongly promotes the dissolution of CO_2 in the melts.

A thermodynamic approach is proposed to predict CO_2 solubility in hydrous silicate melts:

$$x_{CO_{2,total}}^{melt} = (1 + K_2 \cdot x_{O_r^{2-}}^{melt}) \cdot f_{CO_2} \cdot K_1^{o,d} \cdot \exp\left(k \cdot x_{water} + \frac{-V_{CO_{2,mol}}^{melt}(P - P_{ref})}{RT} - \frac{\Delta H_{CO_{2,mol}}^{o}}{R}\left(\frac{1}{T} - \frac{1}{T_{ref}}\right)\right)$$

In this approach an exponential variation of CO_2 solubility with the mole fraction of water in the melt is assumed. The procedure to calculate the CO_2 solubility at given P, T and $x_{CO_2}^{fluid}$ is

(i) estimate the water solubility in the melt for these conditions (e.g., using the model of Tamic et al., 2001, for rhyolitic melts).

(ii) calculate f_{CO_2} for these conditions using the molar volumes and fugacities of pure fluids after Pitzer and Sterner (1994) and activity coefficients for the fluid components after Aranovich and Newton (1999).

(iii) insert the model parameters from Table 6 and the values calculated in (i) and (ii) in the equation above (set $x_{O_r^{2-}}^{melt} = 1$).

Using the data in Table 6 the CO_2 solubility can be calculated for rhyolitic and dacitic melts at high pressure. For intermediate compositions the calculated values may be interpolated using the SiO_2 content. An application of the model at very high $x_{H_2O}^{fluid}$ (>0.9) and very low $x_{CO_2}^{fluid}$ (>0.05) is not recommended because the experimental data do not constrain these ranges. Furthermore, extrapolation of the model to pressures below 100 MPa may have a significant error. Although the temperature dependence of CO_2 solubility was not determined for dacitic melts, an extrapolation towards lower temperature (<1250°C) probably only has a small error. The negligible dissolution enthalpy for CO_2 found for hydrous rhyolitic melts implies that temperature has only a minor influence on CO_2 solubility in silicic melts.

It has to be emphasized that a basic assumption in our modeling is that dissolved water has a direct (reactive) effect on dissolved carbon dioxide. The variation in melt composition by dissolution of water is considered only indirectly by introducing the model parameter *k* to describe the variation of the equilibrium constant K_1 with water content. Hence, our modeling gives insights to the dissolution mechanisms of H_2O and CO_2 for a particular melt composition but the results are not directly transferable to other melt compositions. An alternative is to consider the melt in its whole accounting for interaction between all melt components of the multicomponent liquid. The potential of such a generalized model for predicting H_2O and CO_2 solubilities in silicate melts has been demonstrated by Papale (1999). At present, however, such models suffer from insufficient input data and a direct access to the computation routine is not available.

Acknowledgments— This study was supported by the Deutsche Forschungsgemeinschaft (DFG grant Ho 1337/3+7). Fruitful comments of Hans Keppler, Yang Liu and two anonymous reviewers helped to improve the manuscript.

Associate editor: C. Romano

REFERENCES

Aranovich L. Y. and Newton R. C. (1999) Experimental determination of CO_2-H_2O activity-composition relations at 600–1000°C and 6–14 kbar by reversed decarbonation and dehydration reactions. *Am. Mineral*. **84,** 1319–1332.

Behrens H. (1995) Determination of water solubilities in high-viscosity melts: An experimental study on $NaAlSi_3O_8$ and $KAlSi_3O_8$ melts. *Eur. J. Mineral*. **7,** 905–920.

Behrens H., Romano C., Nowak M., Holtz F., and Dingwell D. B. (1996) Near-infrared spectroscopic determination of water species in glasses of the system $MAlSi_3O_8$ (M = Li,Na,K): An interlaboratory study. *Chem. Geol*. **128,** 41–63.

Behrens H. and Nowak M. (2003) Quantification of water speciation in silicate glasses and melts by IR spectroscopy—In situ vs. quench technique. *Phase Transitions*. **76,** 45–61.

Behrens H. and Stuke A. (2003) Quantification of H_2O contents in silicate glasses using IR spectroscopy—A calibration based on hydrous glasses analyzed by Karl-Fischer titration. *Glass Sci. Techn*. **76,** 176–189.

Behrens H., Tamic N., and Holtz F. (2004) Determination of molar absorption coefficient for the IR absorption band of CO_2 in rhyolitic glasses. *Am. Mineral*. **89,** 301–306.

Berndt J., Liebske C., Holtz F., Freise M., Nowak M., Ziegenbein D., Hurkuck W., and Koepke J. (2002) A combined rapid-quench and H_2-membrane setup for internally heated pressure vessels: Description and application for water solubility in basaltic melts. *Am. Mineral*. **87,** 1717–1730.

Blank J. G. (1993) An experimental investigation of the behaviour of carbon dioxide in rhyolitic melt. Ph.D. diss. California Institute of Technology.

Blank J. G., Stolper E. M., and Carroll M. R. (1993) Solubilities of carbon dioxide and water in rhyolitic melt at 850°C and 750 bars. *Earth Planet. Sci. Lett*. **119,** 27–36.

Blank J. G. and Brooker R. A. (1994) Experimental studies of carbon dioxide in silicate melts: Solubility, speciation and stable isotope behavior. *Rev. Mineral*. **30,** 157–186.

Brenan J. M., Shaw H. F., Ryerson F. J., and Phinney D. L. (1995) Experimental determination of trace-element partitioning between pargasite and a synthetic hydrous andesitic melt. *Earth Planet. Sci. Lett*. **135,** 1–11.

Brooker R. A., Kohn S. C., Holloway J. R., McMillan P. F., and Carroll M. R. (1999) Solubility, speciation and dissolution mechanisms for CO_2 in melts on the $NaAlO_2$-SiO_2 join. *Geochim. Cosmochim. Acta* **63,** 3549–3565.

Brooker R. A., Kohn S. C., Holloway J. R., and McMillan P. F. (2001) Structural controls on the solubility of CO_2 in silicate melts. Part I: Bulk solubility data. *Chem. Geol*. **174,** 225–239.

Chen C.-H., DePaolo D. J., Nakada S., and Shieh Y.-N. (1993) Relationship between eruption volume and neodymium isotopic composition at Unzen volcano. *Nature* **362,** 831–834.

Deloule E., Paillat O., Pichavant M., and Scaillet B. (1995) Ion microprobe determination of water in silicate glasses: Methods and applications. *Chem. Geol*. **125,** 19–28.

Dingwell D. B. and Webb S. L. (1990) Relaxation in silicate melts. *Eur. J. Mineral*. **2,** 427–447.

Dixon J. E., Stolper E. M., and Holloway J. R. (1995) An experimental study of water and carbon dioxide solubilities in mid-ocean ridge basaltic liquids. Part I: Calibration and solubility models. *J. Petrol*. **36,** 1607–1631.

Fine G. and Stolper E. M. (1985) The speciation of carbon dioxide in sodium aluminosilicate glasses. *Contrib. Mineral. Petrol*. **91,** 105–121.

Fogel R. A. and Rutherford M. J. (1990) The solubility of carbon dioxide in rhyolitic melts: A quantitative FTIR study. *Am. Mineral*. **75,** 1311–1326.

Hanon P., Robert F., and Chaussidon M. (1998) High carbon concentrations in meteoritic chondrules:A record of metal-silicate differentiation. *Geochim. Cosmochim. Acta* **62,** 903–913.

Hauri E., Wang J., Dixon J. E., King P. L., Mandeville C., and Newman S. (2002) SIMS analysis of volatiles in silicate glasses 1. Calibration, matrix effects and comparisons with FTIR. *Chem. Geol*. **183,** 99–114.

Hervig R. L., Thomas R. M., and Williams. (1989) Charge neutralization and oxygen isotopic analysis of insulators with the ion microprobe. In *New Frontiers in Stable Isotopic Research: Laser Probes, Ion Probes, and Small-Sample Analysis* (eds. W. C. Shanks III and R. E. Criss), pp 137–143. U.S. Geological Survey.

Hess K. U. and Dingwell D. B. (1996) Viscosities of hydrous leucogranitic melts: A non-Arrhenian model. *Am. Mineral*. **81,** 1297–1300.

Holloway J. R. (1976) Fluids in the evolution of granitic magmas; consequences of finite CO_2 solubility. *Geol. Soc. Am. Bull*. **87,** 1513–1518.

Holloway J. R. (1987) Igneous fluids. *Rev. Mineral*. **17,** 211–232.

Holloway J. R. and Blank J. G. (1994) Application of experimental results to C-O-H species in natural melts. *Rev. Mineral*. **30,** 187–230.

Ihinger P. D., Hervig R. L., and McMillan P. F. (1994) Analytical methods for volatiles in glasses. *Rev. Mineral*. **30,** 67–121.

Jakobsson S. (1997) Solubility of water and carbon dioxide in an icelandite at 1400°C and 10 kilobars. *Contrib. Mineral. Petrol*. **127,** 129–135.

King P. L. and Holloway J. R. (2002) CO_2 solubility and speciation in intermediate (andesitic) melts: The role of H_2O and composition. *Geochim. Cosmochim. Acta* **66,** 1627–1640.

King P. L., Vennemann T. W., Holloway J. R., Hervig R. L., Lowenstern J. B., and Forneris J. F. (2002) Analytical techniques for volatiles: A case study using intermediate (andesitic) glasses. *Am. Mineral*. **87,** 1077–1089.

Kohn S. C., Brooker R. A., and Dupree R. (1991) ^{13}C MAS NMR: A method for studying CO_2 speciation in glasses. *Geochim. Cosmochim. Acta* **55,** 3879–3884.

Kohn S. C. and Brooker R. A. (1994) The effect of water on the solubility and speciation of CO_2 in aluminosilicate glasses along the join SiO_2-$NaAlO_2$. *Min. Mag*. 58A, 489–490.

Kubicki J. D. and Stolper E. M. (1995) Structural role of CO_2 and $[CO_3]^{2-}$ in fully polymerized, sodium-aluminosilicate melts and glasses. *Geochim. Cosmochim. Acta* **59,** 683–698.

Leschik M., Behrens H., Wiedenbeck M., Wagner N., Heide K., Geiβler H., Reinholz U., Heide G., and Frischat G.-H. (2004) Determination of H_2O and D_2O contents in rhyolitic glasses using KFT, NRA, EGA, IR spectroscopy, and SIMS. *Phys. Chem. Glasses,* in press.

Liu Y., Zhang Y., and Behrens H. (2004) Solubility of H_2O in rhyolitic melts at low pressures and a new empirical model to predict H_2O and CO_2 solubility in rhyolitic melts. *J. Volcanol. Geotherm. Res.*,in press.

Mattey D. P. (1991) Carbon dioxide solubility and carbon isotope fractionation in basaltic melt. *Geochim. Cosmochim. Acta* **55,** 3467–3473.

McKeegan K. D., Walker R. M., and Zinner E. (1985) Ion microprobe isotopic measurements of individual interplanetary dust particles. *Geochim. Cosmochim. Acta* **49,** 1971–1987.

Morizet Y., Kohn S. C., and Brooker R. A. (2001) Annealing experiments on CO_2-bearing jadeite glass: An insight into the true temperature dependence of CO_2 speciation in silicate melts. *Min. Mag*. **65,** 701–707.

Morizet Y., Brooker R. A., and Kohn S. C. (2002) CO_2 in haplophonolitic melt: Solubility, speciation and carbonate complexation. *Geochim. Cosmochim. Acta* **66,** 1809–1820.

Mysen B. O., Arculus R. J., and Eggler D. H. (1975) Solubility of carbon dioxide in natural nephelinite, tholeiite and andesite melt to 30 kibar pressure. *Contrib. Mineral. Petrol*. **53,** 227–239.

Mysen B. O., Eggler D. H., Seitz M. G., and Holloway J. R. (1976) Carbon dioxide solubility in silicate melts and crystals. Part I. Solubility measurements. *Am. J. Sci*. **276,** 455–479.

Nowak M., Porbatzki D., Spickenboom K., and Dietrich O. (2003) Carbon dioxide speciation in silicate melts: A restart. *Earth Planet Sci. Lett*. **207,** 131–139.

Ohlhorst S., Behrens H., and Holtz F. (2001) Compositional dependence of molar absorptivities of near-infrared OH- and H_2O bands in rhyolitic to basaltic glasses. *Chem. Geol*. **174,** 5–20.

Pan V., Holloway J. R., and Hervig R. L. (1991) The pressure and temperature dependence of carbon dioxide solubility in tholeiitic basalt melts. *Geochim. Cosmochim. Acta* **55,** 1587–1595.

Papale P. (1999) Modeling of the solubility of a two-component H_2O + CO_2 fluid in silicate liquids. *Am. Mineral*. **84,** 477–492.

Pitzer K. S. and Sterner S. M. (1994) Equation of state valid continuously from zero to extreme pressures for H_2O and CO_2. *J. Chem. Phys*. **102,** 3111–3116.

Reed S. J. B. (1989) Ion microprobe analysis—A review of geological applications. *Mineral. Mag*. **53,** 3–24.

Richet P., Lejeune A. M., Holtz F., and Roux J. (1996) Water and the viscosity of andesitic melts. *Chem. Geol*. **128,** 185–197.

Saxena F. J. and Fei Y. (1987) High pressure and high temperature fluid fugacities. *Geochim. Cosmochim. Acta* **51,** 783–791.

Scherer G. W. (1984) Use of the Adam-Gibbs equation in the analysis of structural relaxation. *J. Am. Ceram. Soc*. **67,** 504–511.

Silver L. A., Ihinger P. D., and Stolper E. (1990) The influence of bulk composition on the speciation of water in silicate glasses. *Contrib. Mineral. Petrol*. **104,** 142–162.

Spera F. J. and Bergman S. C. (1980) Carbon dioxide in igneous petrogenesis: I. Aspects of the dissolution of CO_2 in silicate liquids. *Contrib. Mineral. Petrol*. **74,** 55–66.

Stolper E. M. (1982) Water in silicate glasses: An infrared spectroscopic study. *Contrib. Mineral. Petrol*. **81,** 1–17.

Stolper E. M., Fine G., Johnson T., and Newman S. (1987) Solubility of carbon dioxide in albitic melt. *Am. Mineral*. **72,** 1071–1085.

Storms H. A., Brown K. F., and Stein J. D. (1977) Evaluation of a cesium positive ion source for secondary ion mass spectrometry. *Anal. Chem*. **49,** 2023–2030.

Tamic N., Behrens H., and Holtz F. (2001) The solubility of H_2O and CO_2 in rhyolitic melts in equilibrium with a mixed CO_2-H_2O fluid phase. *Chem. Geol*. **174,** 333–347.

Tingle T. N. (1987) An evaluation of the carbon-14 beta track technique: Implications for solubilities and partition coefficients determined by beta track mapping. *Geochim. Cosmochim. Acta* **51,** 2479–2487.

Watson E. B. (1994) Diffusion in volatile-bearing magmas. *Rev. Mineral*. **30,** 371–411.

Wiedenbeck M., Rocholl A., and Koepke J. (2001) Water—A source of systematic error in quantitative SIMS analyses of hydrous glasses (abstract 3604). LPI Contribution 1088. Lunar and Planetary Science Institute.

Wilson R. G., Stevie F. A., and Magee C. W. (1989) *Secondary Ion Mass Spectrometry: A Practical Handbook for Depth Profiling and Bulk Impurity Analysis*. Wiley-Interscience.

Zhang Y., Stolper E. M., and Ihinger P. D. (1997) Kinetics of reaction $H_2O + O = 2OH$ in rhyolitic glasses: Preliminary results. *Am. Mineral*. **80,** 593–612.

Zhang Y. and Behrens H. (2000) H_2O diffusion in rhyolitic melts and glasses. *Chem. Geol*. **169,** 243–262.

Zinner E., Ming T., and Anders E. (1989) Interstellar SiC in the Murchison and Murray meteorites: Isotopic compostion of Ne, Xe, Si, C and N. *Geochim. Cosmochim. Acta* **53,** 3273–3290.